Comparison of Global Human Modification and Human Footprint Maps

How to cite this document:
Oakleaf, James R. and Christina M. Kennedy. 2018. Comparison of global Human Modification and Human Footprint maps. Conservation Gateway, The Nature Conservancy. Available at:
http://www.conservationgateway.org/ConservationPractices/lands/science/publications/Documents/HM_HF_comparison_documentation.pdf

Overview of the comparison of global maps on the human influence on terrestrial lands
To date, the most frequently cited and relied upon map on the influence of human activities globally is the Human Footprint (HF) (Sanderson *et al.*, 2002).[1] The HF is an index of human pressure on terrestrial lands, and conversely identified the "last of the wild", based on a summation of eight global data layers on 1) human population density, 2) built-up areas, 3) cropland, 4) pastureland, 5) night-time lights, 6) roads, 7) railroads and 8) navigable rivers. The HF map was originally created using data sources that reflected the land status of early 1990s, and recently updated to ~2009 using a similar methodology (Venter *et al.*, 2016b).[2]

An alternative approach to mapping terrestrial human influence has been put forth and applied in the U.S. (Theobald, 2010, Theobald, 2013, Theobald *et al.*, 2016), called the human modification (HM) model. This model captures similar ecological stressors as the HF (e.g., human settlement, non-natural cover types, and roads),[3] but is based on an existing threat classification system (Salafsky *et al.*, 2008). The HM produces a cumulative metric based on mapping the spatial extent and intensity of a human activity to derive a continuous 0-1 metric that reflects the proportion of a landscape modified by humans. Kennedy *et al.* (2019) tailored this approach to map the cumulative degree of human modification of terrestrial lands globally at a 1-km resolution (referred to as the *HM$_c$* map), which is publicly available on figshare (Kennedy *et al.*, 2018).

To understand the differences in the outputs of these two maps, we compared the HF and *HM$_c$* datasets and methodologies. Key differences between the HF and *HM$_c$* methodologies are summarized below and in Table 1, with additional information in subsequent sections. See also Kennedy *et al.* (2019) and Venter *et al.* (2016b) for further details on methodological approaches underlying the *HM$_c$* and HF maps, respectively.

    (i) **Output resolution:** Both maps were produced at 1 km resolution. The *HM$_c$* map included input datasets that were produced at 1 km or finer resolution to minimize the over-estimation of human impacts due to stressor values being uniformly mapped at coarser scales (Halpern & Fujita, 2013). The 2009 HF map included datasets at coarser native resolutions (i.e., ~4 km^2 for human population, 10 km^2 for pasture), which were then downscaled to 1 km^2 to allow for temporal comparison with the earlier 1993 map.

---

[1] Available at: http://sedac.ciesin.columbia.edu/data/set/wildareas-v2-human-footprint-geographic
[2] Available at: http://datadryad.org/resource/doi:10.5061/dryad.052q5
[3] The HF framework refers to human activities with the potential to impact or harm natural systems as "pressures", whereas they are referred to as ecological "stressors" in the HM framework. Both can be considered synonymous and provide a measure of the human influence (disturbance or modification) of terrestrial lands.

(ii) **Temporal date:** Source dates of input stressor datasets varied with the HM_c map being of more recent land status. The median date of the input datasets for the HF map was 2009 (mean ± 1 SD = 2006 ± 3.9), whereas it was 2016 (mean = 2014 ± 2.9) for the HM_c map. The HM_c map used the most recent data to capture contemporary land status, whereas the HF used data sources that allowed for consistent stressors across different time periods (i.e., 1993 and 2009) (Venter *et al.*, 2016b).

(iii) **Human stressors included:** HF included 8 stressor datasets (human population density, built-up areas, cropland, pastureland, roads, railroads, navigable rivers, and night-time lights). HM_c included 13 stressor datasets (human population density, built-up areas, cropland, livestock density, major roads, minor roads, two-tracks, railroads, mines, oil wells, wind turbines, powerlines, and night-time lights). For further details on these datasets, see respective sections below in "Comparison of the stressors".

(iv) **Calculation of a spatial extent.** HF treated stressor layers as binary and assumed that each cell with a stressor was fully occupied, regardless of the input resolution. This approach may cause the final HF scores to overestimate physical footprints and be driven by their stressor weightings. The HM_c calculated the spatial extent based on the proportion of converted land for built-up areas, cropland, roads, powerlines, oil wells, wind turbines, mines, and the log[X+1] transformed values for human population, livestock numbers, and night-time lights. HM spatial extents (H_e) ranged from 0.00 to 1.00 on continuous scale.

(v) **Treatment of human access.** The potential indirect effects of humans encroaching from conduits such as roads, navigable waterways, and coastlines were accounted for in the HF by buffering and applying an exponential distance decay effect 15 km from these features. This approach causes roads to have an over-riding effect on the spatial distributions of land patterns. Such indirect effects were not factored into the HM_c, which focused on mapping the direct spatial extents of human activities.

(vi) **Weighting of stressors.** HF adopted a scoring system whereby each stressor was assigned a score (or weight) ranging from 0 to 10 that was largely categorical based on expert opinion, as described in (Sanderson *et al.*, 2002). In the HM_c map, HM_s values for each stressor, s, were multiplied by its potential intensity of impact scaled from 0.00 to 1.00. Intensity values (HM_i) were determined from generalized land use coefficients that measure the intensity of a human activity based on the amount of different forms of energy and resources (e.g. water, fossil fuels, fertilizers, electricity, minerals, etc.) required to maintain it, termed emergy (Brown & Ulgiati, 2002, Brown & Vivas, 2005).

(vii) **Aggregation of stressors into a cumulative score.** In the HF, scores were summed together for each 1-km² cell to produce a cumulative score that ranged from 0 to 50. The assumption under this method is that multiple, overlapping stressor effects are additive. The HM_c values per stressor were continuous ranges from 0.00 to 1.00 and aggregated into the cumulative HM_c using the fuzzy algebraic sum (Bonham-Carter, 1994). This algorithm produced an increasive effect, whereby an area experiencing multiple stressors is given a higher modification score than those with a single stressor; but the additional

contribution decreases as values from other stressors overlap and ultimately converge to 1.00. This approach accounts for cumulative effects of multiple stressors in a way that minimizes the bias associated with non-independent stressor layers and is robust to the addition of stressors as new data become available (Perkl, 2017). It also assumes that multiple human-induced stressors tend to be accumulative (i.e., greater than just the dominant stressor) but non-additive (and specifically, antagonistic), which has support in the empirical literature (Crain *et al.*, 2008, Darling & Côté, 2008).

(viii) **Accounting for parameter uncertainty.** A source of uncertainty in both assessments is the weights or intensity values ascribed to each stressor. This uncertainty was assessed in a national-level sensitivity analysis by randomly perturbing the weighting for each pressure score up by 50% and down by 50% or keeping it the same (with this procedure repeated 100 times) (Venter *et al.*, 2016a). This uncertainty was accounted for by randomly selecting intensity values using a uniform distribution between a reported minimum and maximum range for each stressor. This perturbation was repeated 100 times to produce 100 cumulative HM_c values that were then averaged to derive the value for each 1-km^2 area in the final HM_c map.

(ix) **Validation.** Both datasets were subject to validation based on visual interpretation of high resolution satellite imagery. For the HF, stressors (i.e., built-up areas, crop lands, pasture lands, roads, human settlements, infrastructures and navigable waterways) were recorded for 3,114 1-km^2 plots using a standard key and attributed a categorical score from 0 (none), 1 (sparse, <12%), 2 (medium, >12.5%), and 3 (dense, >50%). The degree of HM_c was visually interpreted at 10,000 random sub-plots within 1,000 plots (~600 m x 600 m) on a 0 – 100 range using the Global Land Use Emergent Database protocol (Theobald, 2016) and based on the lowest-highest-best estimate elicitation procedure to reduce expert assessment biases (McBride *et al.*, 2012, Speirs-Bridge *et al.*, 2010). The average error was estimated to be ~13% RMSE for the HF and ~14% MAE for the HM_c. 88.5 % of HF plots and 71% of HM_c plots were found to be within 20% agreement between the visual and mapped values. We note that the estimated error is expected to be lower for the HF map relative to the HM_c map, given that the former consisted of categorical scores within narrower ranges (0 – 11 for visual scores and 0 – 50 for mapped scores) relative to the latter with a continuous range from 0 – 100 (for both visual and mapped scores).

(x) **Differences in final scores.** While the HF and HM_c maps were strongly correlated, HM_c values tended to be higher than HF values. Specifically, ~25% of comparable cells had higher HM_c values relative to only 5% of HF values. Mean and median scores by country, ecoregion, and biome were also correlated between the two datasets, but the HM_c values were consistently estimated to be higher. Despite high correlations at broad scales (i.e., global, biome, ecoregion, and country), spatial distributions of scores varied substantially within a given region. The HF map delineated 3.7 times more areas devoid of human stressors (i.e., HF = 0). The HF mapped ~19% of terrestrial lands without human influence relative to ~5% by the HM_c map. The main stressors found to drive differences were human population density, navigable waterways, roads, cropland, livestock densities, and pasture. The way in which the different stressor scores were

aggregated also influenced differences between cumulative HF and HM_c values. Refer to subsequent sections on the comparisons between HM_c values and HF scores for further details.

Table 1. Attributes of Human Footprint (HF) and Human Modification (HM_c) methodology.

Category	HF	HM_c
Name	Human Footprint	Human Modification
Resolution	1 km (2 datasets downscaled from 4 km, 10 km resolution)	1 km (all input datasets at 1 km native resolution or finer)
Primary stressor datasets	8 (human population density, built up areas, cropland, pasture, major roads, railroads, navigable rivers, night-time lights)	13 (human population density, built-up areas, cropland, livestock density, major roads, minor roads, two-tracks, railroads, mines, oil wells, wind turbines, powerlines, night-time lights)
Source dates for stressor datasets (# of datasets)	2000 (2), 2005(1), 2009 (4), 2010 (1)	2005 (1), 2013 (1), 2014 (2), 2015 (1), 2016 (8)
Calculation of footprint	Treated each stressor layer as binary and assumed that each cell with a stressor was fully occupied (value = 1)	Determined the proportion of the cell modified by each stressor per 1-km^2 area (values ranged from 0 to 1)
Indirect effects due to human access	Accounted for by applying distance decay effect 15 km from roads, navigable waterways, and coastlines	Not included
Values per stressor	Assigned scores from 0 – 10, mostly categorical	Footprint or Stress level x Intensity, continuous from 0 to 1
Cumulative score	Summation of cell values	Applied Fuzzy Sum algorithm
Range of output values	0 (none) – 50 (high)	0 (none) – 1 (high)
Uncertainty techniques employed	Sensitivity analysis at national-level assessment	Uniform random selection of intensity values between min and max values, with 100 permutations, integrated into final map
Technical validation	Yes	Yes

Comparison of individual stressors

Despite an overlap in categories of human stressors, there were differences in the source data layers used and how they were processed to derive scores under the different analyses (Table 2).

First, although both the HM_c and HF maps were produced at a 1-km resolution, the HM_c restricted inclusion of data layers to those produced at this same resolution or finer. This was done to minimize the over-estimation of human impacts due to stressor values being uniformly

mapped at coarser scales (Halpern & Fujita, 2013). The HF included datasets at coarser native resolutions (i.e., ~4 km^2 for human population, 10 km^2 for pasture), which were then downscaled to 1 km^2. This allowed for the integration of pressures in the HF map that were only available at coarser resolutions.

Second, the temporal dates of the source data layers were more recent in the HM_c: median for the HF map was 2009 (mean ± 1 SD= 2006 ± 3.9), whereas it was 2016 (mean = 2014 ± 2.9) for the HM_c map (Table 1).

Third, the number and type of stressor data layers varied between the two maps. The HF included 8 stressors, of which navigable waters was one that unique to this analysis. The HM_c included 13 stressors, of which mining, oil wells, wind turbines, and powerlines were unique. While the HF only included major roads, the HM_c included three road types (i.e., major, minor, and unimproved). To capture rangeland activities, the HF included a pasture layer whereas the HM_c included a livestock density layer. See the related sections below for further details on the differences between comparable stressors.

Table 2. Stressors included in the HF and HM_c maps with their associated input data sources and dates, resolutions (or positional accuracy), processing techniques, and scoring methods.

Stressor	HF Data Source - Date	Res. (km)	HF – Data processing	HF – Potential Score	HM_c Data Source -Date	Res. (km)	HM_c – Data processing	HM_c – Potential Score*
Human Population Density	Gridded Pop of World v3 - 2010	~4	1. Assigned all PD $\geq$ 1000/km^2 to 1000 2. Log (PD+1) * 3.333 3. Rounded to nearest integer	0-10 (integers)	Gridded Pop of World v4 - 2015 UN adjusted estimate	1	1. Assigned all PD $\geq$ 4,246 /km^2 to 4,246 2. Calculated log(PD+1) 3. Max normalized to 1	0-0.5
Built-up Areas	Night-time lights (DMSP-OLS) - 2009	1	1. Select cells with DN > 20 2. Assign value of 10	0 or 10	Global Human Settlement Layer -2014	0.3	1. Calculate mean proportion built-up at 1km	0-1.0
Cropland	GlobCover - 2009	0.3	1. Select cropland cells 2. Assign value of 7	0 or 7	Unified Cropland Layer - 2014	0.25	1. Calculate mean proportion cropland at 1km	0-0.7
Pasture /Grazing	Pasture Lands - 2000	10	1. Max normalize percent pasture to 4 2. Round to nearest integer	0 - 4 (integers)	Gridded Livestock of the World V2 - 2005	1	1. Calculate livestock units (LU) for sheep, goats, cows 2. Assigned all LU $\geq$ 1,000 /km^2 to 1,000 3. Log(LU+1) 4. Max normalize to 1	0-0.37
Roads	gRoads - 2000	($\pm$ 500 m)	1. Create 1 km raster with values of 8 2. Assign cells from 4 - 0 based on exponential decay function from cells adjacent to roads up to 15 km	0 or 8 0-4 (floating)	Major, Minor, Unimproved/4 w-drive Roads Open Street Map (OSM) – 2016; supplemented with gRoads – 2000	($\pm$ 500m, 20 m)	1. Calculated road density per 1 km^2 for each category 2. Multiplied density by road widths (i.e., 30m, 15m, 3m) 3. Calculate road proportion of cell for each category	Major: 0 - 0.83 (0.622)** Minor: 0 – 0.50 (0.475)** Two-tracks: 0 – 0.2 (0.0272)**
Railways	VMAP0 - 2000	($\pm$ 500 m)	1. Create 1 km raster with values of 8	0 or 8	OSM – 2016; supplemented with VMAP0 - 2000	($\pm$ 500m, 20 m)	1. Calculated rail density per km^2 2. Multiplied density by rail width of 10m 3. Calculate rail proportion of cell	0 – 0.83
Navigable Waters	Hydrosheds - 2016	1	1. Select all major rivers (formula used to select) and coastline banks	0 – 4 (floating)	NA	NA	NA	NA

			within 80 km of a bank with night-time lights (DNI > 6) at least 4 km form bank 2. Assign cells from 4 -0 based on exponential decay function from bank cells up to 15 km					
Industrial & Mining	NA	NA	NA	NA	OSM - 2016	100 m (± 20 m)	1. Converted polygons to 100m raster based on cell majority 2. Calculated proportion of 1km covered by 100m mining cells	0 - 1
Powerlines	NA	NA	NA	NA	OSM – 2016; supplemented with VMAP0 - 2000	(± 500m, 20 m)	1. Calculated powerline density per km^2 2. Multiplied density by powerline width of 15m 3. Calculate powerline proportion of cell	0 – 0.2 (0.094)**
Oil Wells	NA	NA	NA	NA	OSM - 2016	(± 20 m)	1. Counted number of points per km cell 2. Multiplied count by footprint size 1.4 ha 3. Calculate well footprint proportion of cell	0 – 1.0 (0.63)**
Wind Turbines	NA	NA	NA	NA	OSM - 2016	(± 20 m)	1. Counted number of points per km cell 2. Multiplied count by footprint size 0.14 ha 3. Calculate turbine footprint proportion of cell	0 – 0.5 (0.128)**
Night-time Lights	Night-time lights (DMSP-OLS) - 2009	1	1. Select cells with DN > 6 2. Categorized into 10 equal area (quantile) bins	0 – 10 (integers)	Night-time lights (DMSP-OLS) - 2013	1	1. Calculated log(DN+1) 2. Max normalize to 1	0 – 0.5

* HM_c values are calculated as spatial extent multiplied by intensity for each stressor. Spatial extents range from 0 to 1 but have lower max values than 1 because these values were multiplied by intensity values.

**Numbers in parentheses are top values based on the calculated global footprint values for that stressor and then multiplied by a respective maximum intensity value.

Human Population Density

For human population density, both assessments used the Gridded Population of the World dataset, but with different temporal UN adjusted values (2010 for HF and 2015 for HM) (Doxsey-Whitfield *et al.*, 2015). The differences in the temporal date, resolution of the input layers (i.e., ~4 km vs 1 km), and the valuation led to scores varying at both global and regional scales (Fig.1, top panel). At a regional scale (Fig. 1 bottom panel), the HM_c values exhibited higher granularity than HF values. This is expected to result in an overestimate in the extent of populated areas for those categories identified by the HF. Globally, the HF had scores greater than zero for 83,648,065 cells (i.e., 62% of the analysis extent), which is lower than the HM_c with 118,621,322 cells (i.e., 88% of the analysis extent). This difference, however, had little detectable influence on the cumulative score, because 95% of cells were assigned a HF population score = 0 and HM_c score > 0 had values less than 0.1. The max potential score for this stressor was 10 (out of 10) for the HF and 0.5 (out of 1.0) for the HM_c (Table 2). In both assessments, max pressure (for HF) or intensity (for HM) scores were allocated to areas with the following thresholds for population densities: 1000 people/km^2 for the HF versus 4246 people/km^2 for the HM_c. As a result, a greater number of the HF cells were ascribed maximum scores (i.e., 10). However, in the summation approach used by the HF (after 0-1 normalization), the maximum contribution of this stressor was 0.2 (i.e., 10/50).
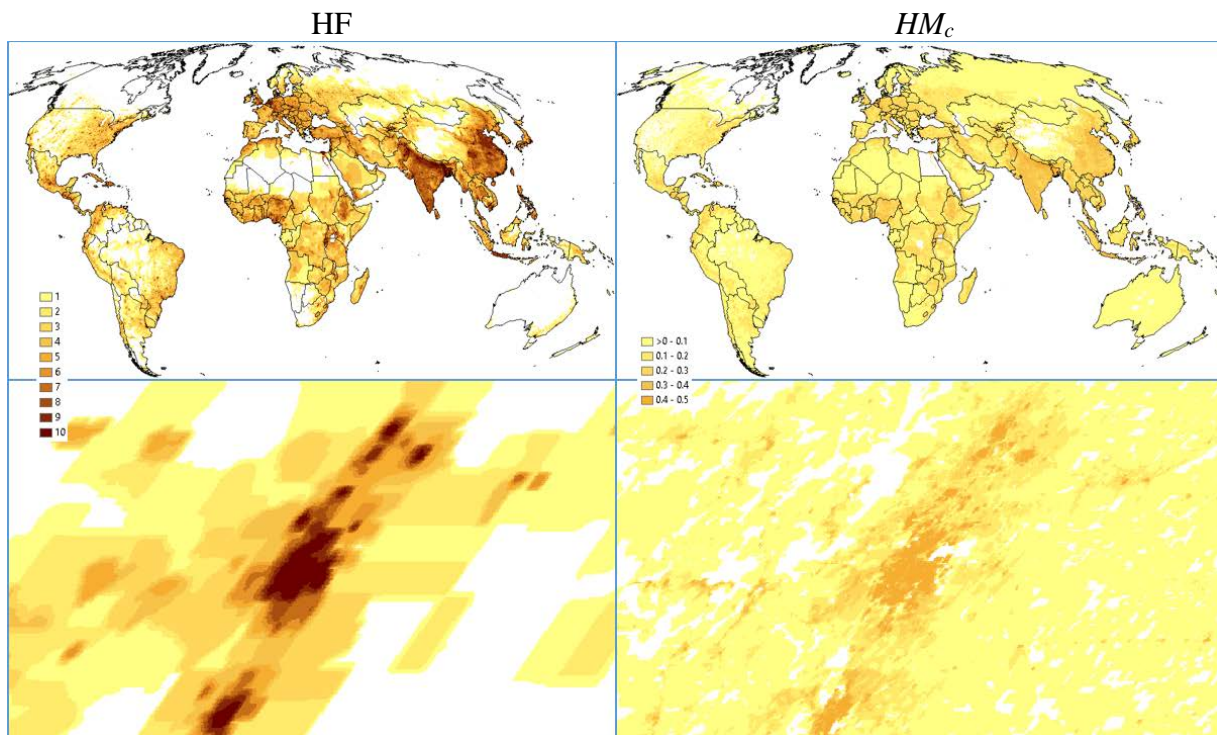

Figure 1. Human population maps for HF globally (top-left) and Denver, CO, USA (bottom-left); and *HM_c* globally (top-right) and Denver, CO, USA (bottom-right). Dark brown values denote the highest and light yellow the lowest values in each map (zero values shown in white).

Built-up areas

Built-up areas were mapped using different input datasets. The HF relied on night-time lights (Elvidge *et al.*, 2001), and designated all areas with DN values > 20 as built-up with a pressure score of 10 (Table 2). In contrast, the HM_c mapped the proportion of "built-up" areas based on the Global Human Settlements Layer (GHSL), which identifies the percent of buildings or structures at 300-m resolution (Pesaresi *et al.*, 2013). Based on these different approaches, the HF designated cells as fully built-up although variation exists (Fig. 2). Globally, the HF classified 2,503,208 cells (i.e., 2% of the analysis extent) as built-up, whereas the HM_c identified 12,550,222 cells (i.e., 9%) with some proportion of built-up. Nearly 80% of built-up cells fell below a HM_c score of 0.1 (or 10% of the km^2 cell classified as built-up), and only 3,960 cells (i.e., 0.003%) had a value of 1 (or 100% built-up). Under the different scoring methods, the contribution of this stressor could range from 0 to 1 under HM, and 0 or 10 under HF (Table 2). This results in a normalized value of only 0.2 (10/50) in the overall cumulative score under the HF, as opposed to 1.0 under the HM.
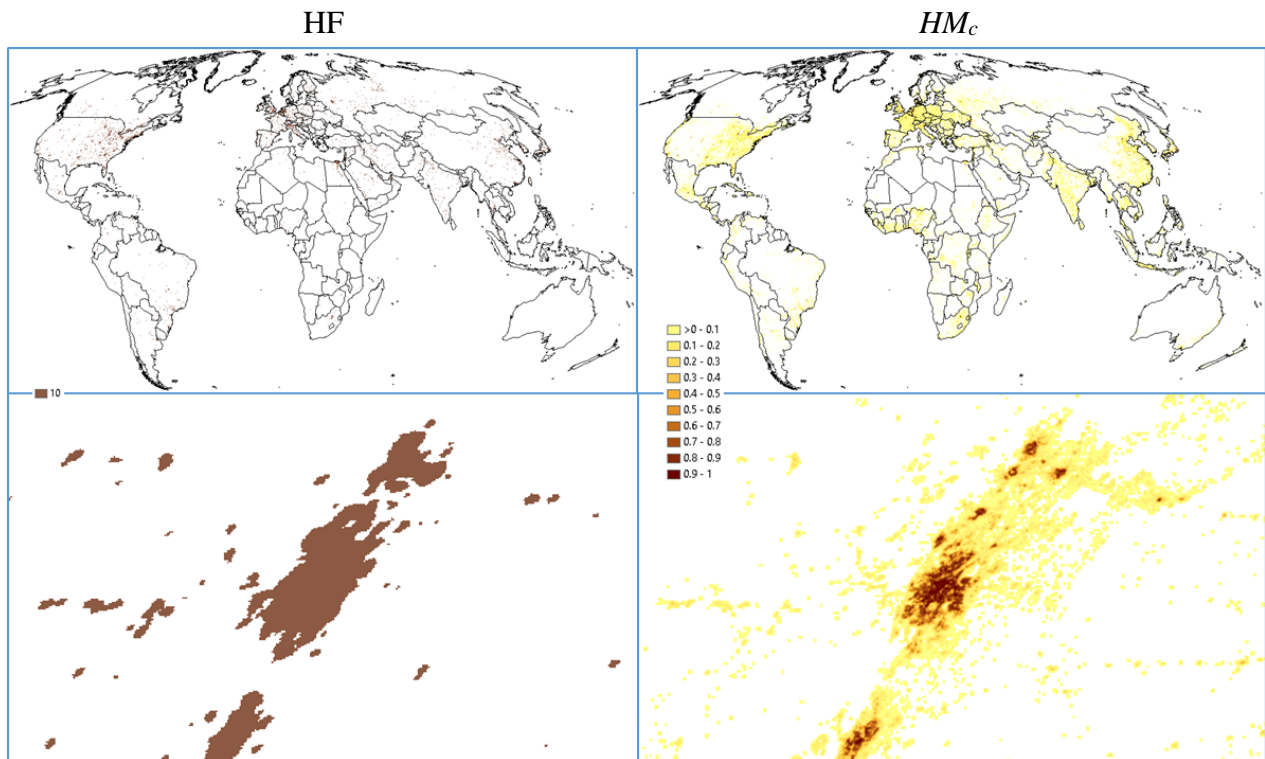

Figure 2. Built-up maps for HF globally (top-left) and Denver, CO, USA (bottom-left); and HM_c globally (top-right) and Denver, CO, USA (bottom-right). Dark brown values denote the highest and light yellow the lowest values in each map (zero values shown in white).

Cropland

Similar to built-up areas, cropland was also mapped using different input datasets. The HF mapped cropland based on agricultural land cover identified by GlobCover (European Space Agency, 2011), and assigned these areas with a uniform pressure score of 7 (out of 10). In contrast, the HM_c mapped a continuous proportion of cropland within a 1-km^2 cell using the Unified Cropland Layer. This dataset identifies the percentage of annually cultivated areas at a 250-m resolution by harmonizing existing global, regional, and national datasets (Waldner *et al.*, 2016).[4] Deriving HM_c values from the proportion identified as cropland provided greater heterogeneity in this stressor relative to HF (Fig. 3). Globally, the HF classified 18,336,348 cells (14%) as cropland, whereas the HM_c classified 29,931,668 cells (22%) comprised of some proportion of cropland. Approximately 16% of HM_c cells or 4% of cells globally (i.e., 4,917,937 cells) had the highest score of 0.7 or 100% cropland for the entire 1km^2 area.
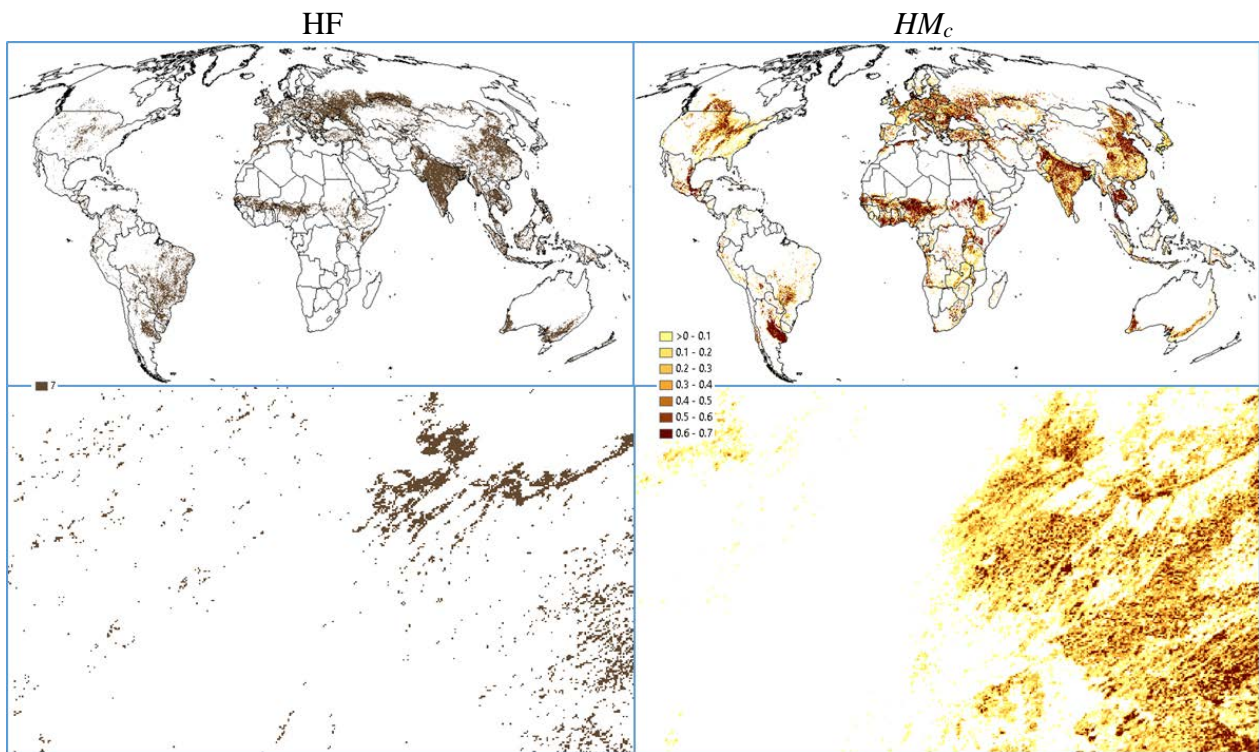

Figure 3. Cropland maps for HF globally (top-left) and Denver, CO, USA (bottom-left); and HM_c globally (top-right) and Denver, CO, USA (bottom-right). Dark brown values denote the highest and light yellow the lowest values in each map (zero values shown in white).

---

[4] Of note, for the HM map, we assessed several different datasets for cropland, including GlobCov. Based on visual assessment, the Unified Cropland Layer was found to better represent global cropland extent, especially in areas of mixed land use with grasslands or meadows.

Pasture/Grazing

To gauge the impact of grazing, the HF relied on the only dataset available on global extent of pasture lands (Ramankutty *et al.*, 2008).[5] In contrast, the HM_c relied on the Gridded Livestock of the World v2 database that indicates the intensity of grazing by censuses of the cattle, sheep, and goats per 1-km^2 (Robinson *et al.*, 2014). Unsurprisingly, the use of different datasets resulted in different spatial distributions of pasture or grazing (Fig. 4). In both the HF and the HM, the pressure weights (or intensity values) ascribed to either pasture or grazing was relatively low (HF: 0.4, HM: 0.2-0.37), resulting in this stressor having a similar range of possible scores under the two maps (Table 2).[6] Thus, the differences in the datasets underlying this stressor were not detected to produce substantial overall differences in cumulative scores, except on the low end of the spectrum.
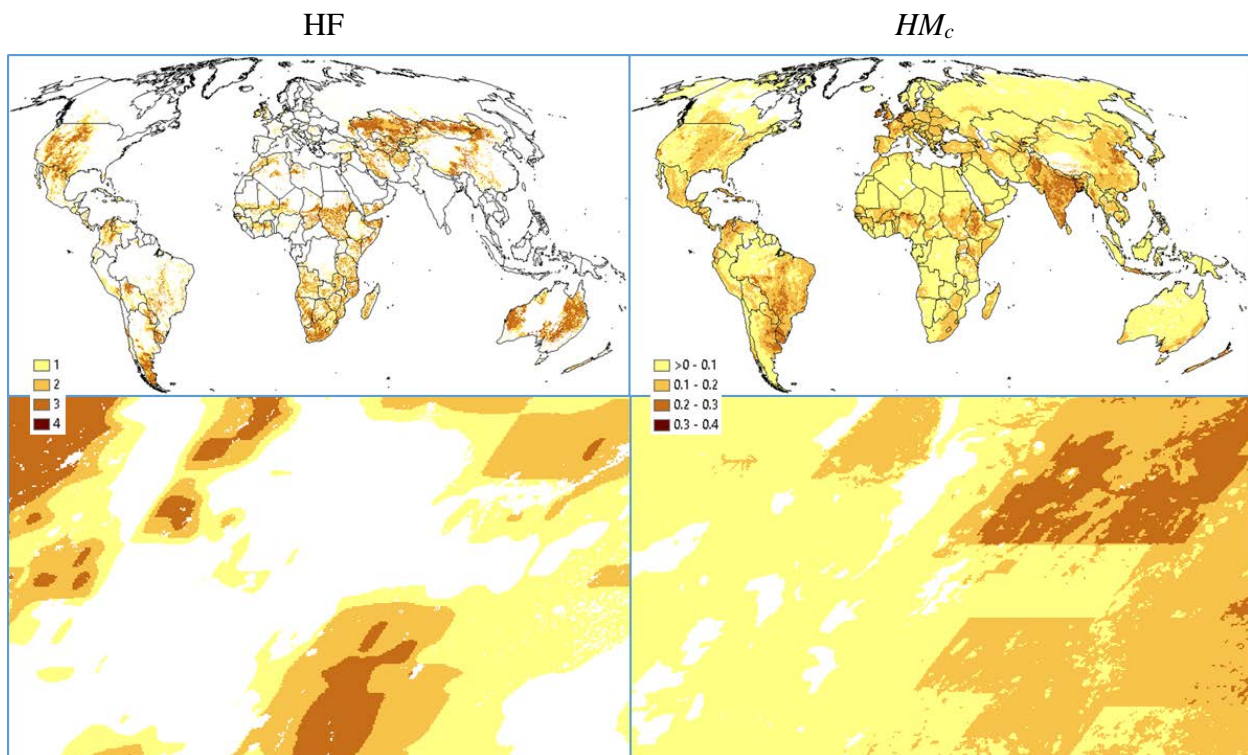

Figure 4. Pasture/grazing maps for HF globally (top-left) and Denver, CO, USA (bottom-left); and *HM$_c$* globally (top-right) and Denver, CO, USA (bottom-right). Dark brown values denote the highest and light yellow the lowest values in each map (zero values shown in white).

---

[5] For the HM, we did not include the Ramankutty *et al* (2008) dataset because it had a native resolution of 10 km and an estimated ground-date of 2000.

[6] Of note, the HM intensity values likely underestimate impacts of intense grazing/feedlots given that they can cause substantially more environmental damage than an area fully identified as pasture land.

Roads

To gauge the impacts of roads, the HF and HM_c used different datasets and scoring approaches. While both used gRoads v1 (Center for International Earth Science Information Network - CIESIN - Columbia University and Information Technology Outreach Services - ITOS - University of Georgia, 2013), this dataset was the only source for roads in the HF, whereas it was used as a supplemented to OpenStreetMap (OSM) (OpenStreetMap contributors, 2016) in the HM. The HF mapped only major roads, whereas the HM_c mapped major roads, minor roads, and two-tracks. In their scoring approaches, the HF accounted for both direct and indirect influences of roads, whereas the HM_c mapped only direct footprints. For direct influences, the HF assigned a pressure score of 8 to all 1-km^2 cells where major roads intersected (thereby affecting 10,028,197 cells, or 7% of terrestrial lands). For indirect influences, the HF assigned a pressure score of 4 and then applied an exponential decay function out to 15 km of either side of a road (thereby affecting 81,759,749 cells, or 60% of terrestrial lands). In contrast, the HM_c estimated the total proportion of roads for each 1-km^2 cell by calculating linear densities of each road type and then multiplying typical road widths (i.e., 30 m for major roads, 15 m for minor roads, and 3 m for two-tracks). These road footprints were then multiplied by their estimated relative range of intensities (major roads: 0.78-0.83, minor roads: 0.39-0.50, two-tracks: 0.10-0.20). Globally, HM_c identified 25,877,603 cells (or 19% of terrestrial lands) with some proportion of roads. Only those cells with dense road networks were scored to have the highest HM_c value (i.e., 0.63); and 98% of cells had cumulative road values < 0.1. This produced very different distributions of road impact values both globally and regionally (Fig. 5), which influenced overall cumulative scores for the two final maps.
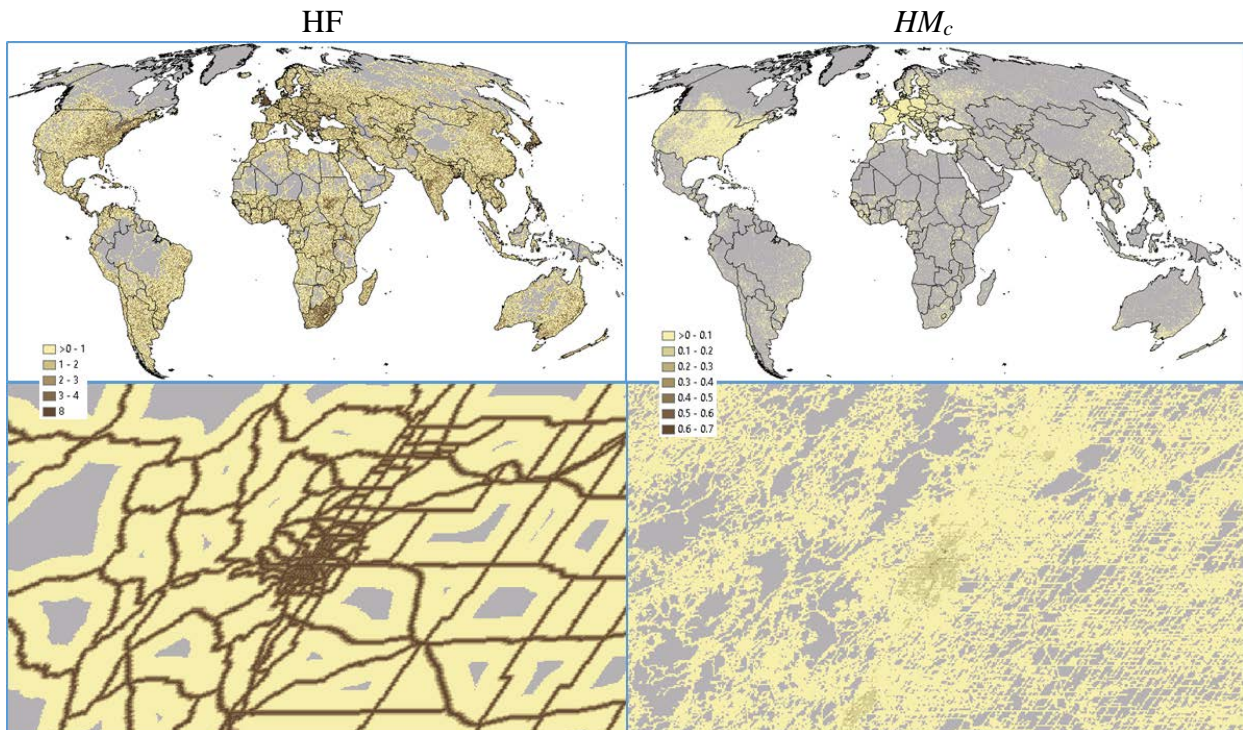
HF HM_c

Figure 5. Roads maps for HF globally (top-left) and Denver, CO, USA (bottom-left); and *HM_c* globally (top-right) and Denver, CO, USA (bottom-right). Dark brown values denote the highest and light yellow the lowest values in each map (zero values shown in white).

Railroads

Similar to roads, the HF and HM_c used different datasets and scoring approaches for railroads. Both the HF and HM_c used Digital Chart of the World (DCW) vMap0 data (National Imagery and Mapping Agency, 1992), but only HM_c supplemented this with OSM data (where available). The HF assigned a pressure score 8 to all 1-km^2 cells intersecting a railroad. As done for roads, the HM_c estimated the proportion of each 1-km^2 cell impacted by railroad based on a linear density multiplied by a footprint (10 m width). These proportions were then multiplied by an intensity estimate (ranging from 0.78-0.83). The HF identified 2,555,926 cells with railroads (or 1.9 % of terrestrial lands) relative to 1,738,282 cells (or 1.3%) under the HM_c. Over 99% of HM_c cells had a score < 0.1 whereas all HF railroad cells had a normalized score of 0.16 (8/50). Thus, while the spatial distributions of railroads were more similar than for roads (Fig. 6), the differences in the mapped footprints and in scoring approaches led HF to give more weight to this stressor than the HM_c in the overall cumulative score.

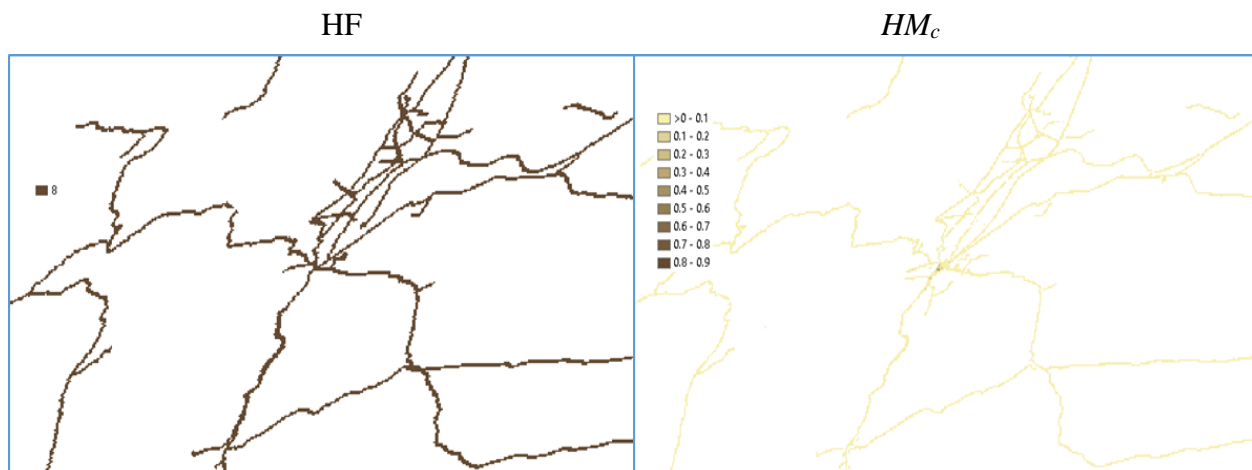HF HM_c

Figure 6. Railroads maps for HF for Denver, CO, USA (left) and HM_c for Denver, CO, USA (right). Dark brown values denote the highest and light yellow the lowest values in each map (zero values shown in white). Global map not provided because railways were not discernable at that scale.

Night-time Lights

Both HF and HM_c used night-time lights to indicate impacts from human electrical infrastructure, which was based on the same dataset but different sources dates (i.e., DMSP-OLS 2009 for HF and 2013 for HM) (Elvidge *et al.*, 2001). Unlike in the HM_c where the continuous distribution of DN values were used, the HF excluded low-lit areas (identified as DN <=6) and then binned remaining values into 10 equal quantile bins. These differences led to different spatial distributions of this stressor (Fig. 7). Globally, the HF scored 9,845,537 cells (or 7% of terrestrial lands) as having some level of night-time lights, whereas the HM_c identified 19,771,406 cells (15%). Based on different pressure scores (1-10) or intensity values (0-0.5), the maximum contribution of this stressor to overall cumulative scores were 0.2 (10/50) for HF and 0.5 for HM_c.
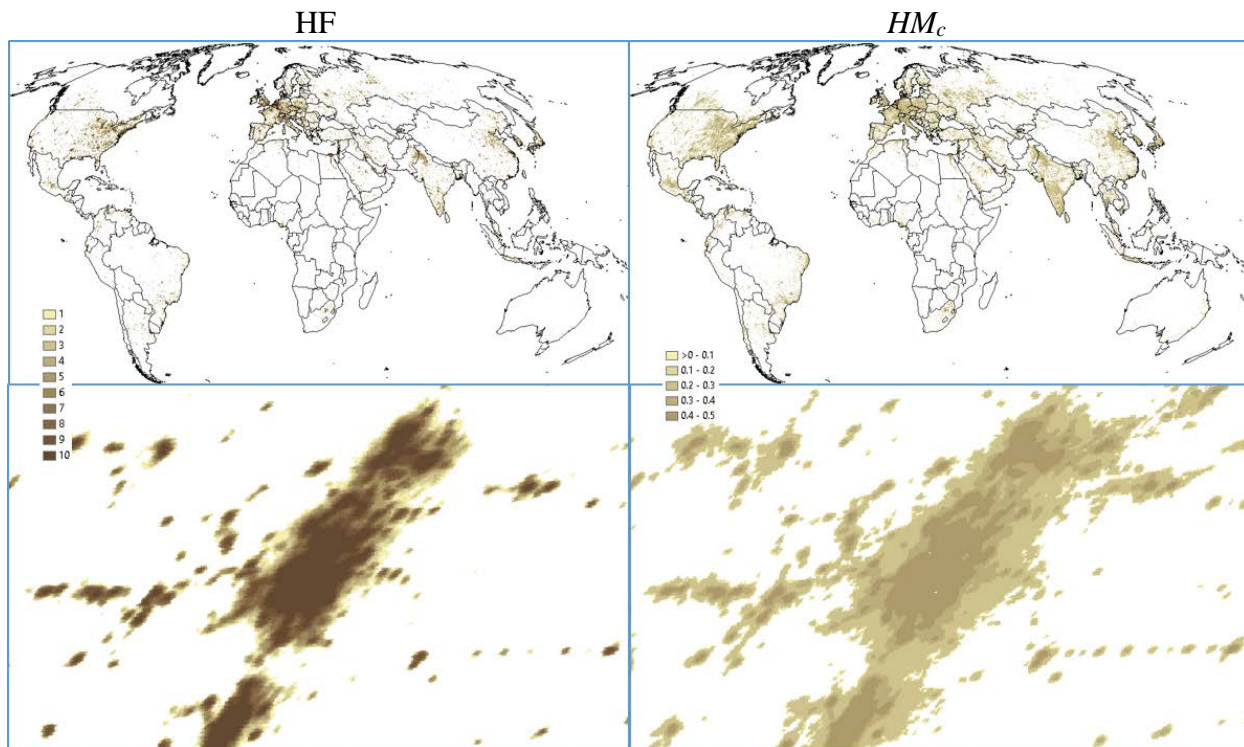

Figure 7. Night-time lights maps for HF globally (top-left) and Denver, CO, USA (bottom-left); and HM_c globally (top-right) and Denver, CO, USA (bottom-right). Dark brown values denote the highest and light yellow the lowest values in each map (zero values shown in white).

Stressors not included in both analyses and thus no comparison is provided.
- *HF – Navigable Waters*
- *HM_c – Mining/Industrial, Powerlines, Wind Turbines, and Oil Wells*

Comparison of HM_c values and normalized HF scores

To compare the two maps on a cell by cell basis, we first aligned the HF raster cells to the HM_c raster cells. This required a vertical shift of 270 m north by the HF cells and no shift horizontally (i.e., east – west).[7] We then selected only those cells that had a value for both HF and HM_c. This removed 882,403 cells and 1,005,650 cells from the HF and HM_c datasets, respectively; and maintained 133,181,983 cells for comparison. The two maps had a different number of scored cells due to the way in which they defined and mapped terrestrial lands and treated inland waters. For example, the HM_c dataset excluded all cells classified as fully inundated by either freshwater or saltwater, whereas many inland water bodies were included in the HF dataset. Additionally, the HM_c analysis included all 1-km^2 cell with $\geq$ 62.5 ha of land (i.e., 1/16 of sq. km), which allowed greater inclusion of coastlines than detected for HF. Finally, to allow for score comparison, we rescaled the HF from 0-50 to 0-1 by applying a maximum normalization calculation. This process created maps with equal aerial extent and attributed comparable cell values across terrestrial lands for HM_c (Fig. 8) and HF (Fig. 9).
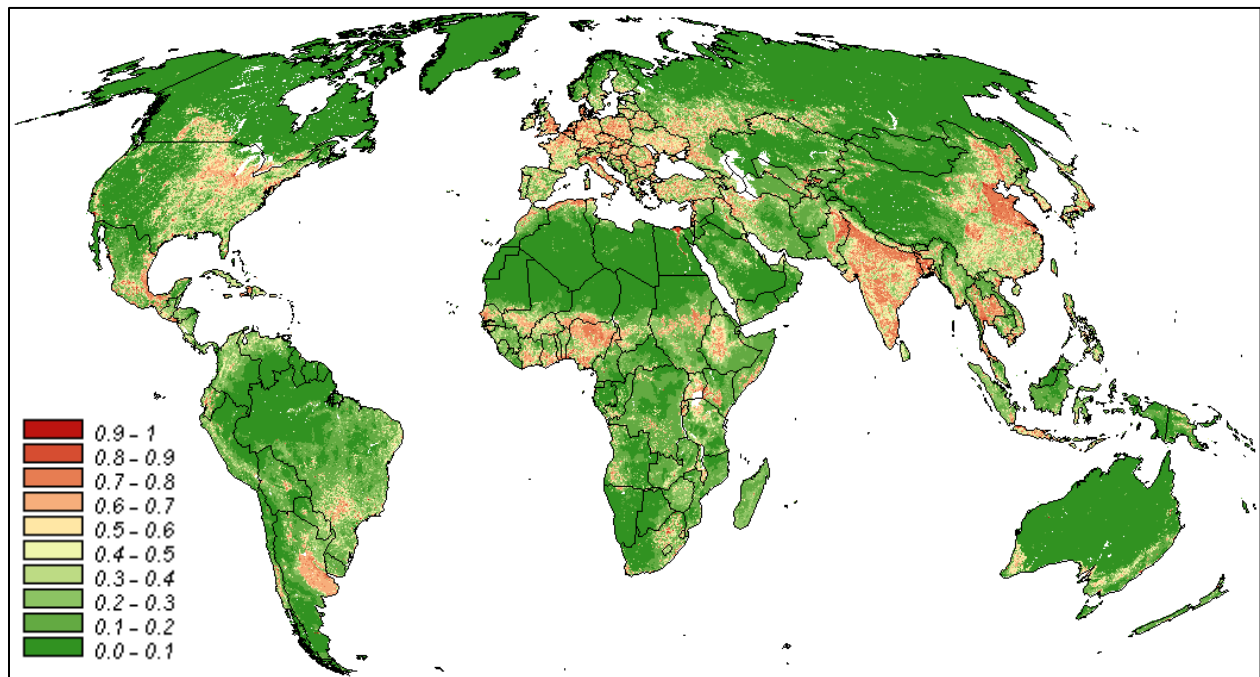

Figure 8. The HM_c map displayed in equal interval bins.

---

[7] Both datasets were in Mollweide projection at a 1-km resolution; thus, reprojecting or resampling modifications were not required (thereby eliminating related distortions).
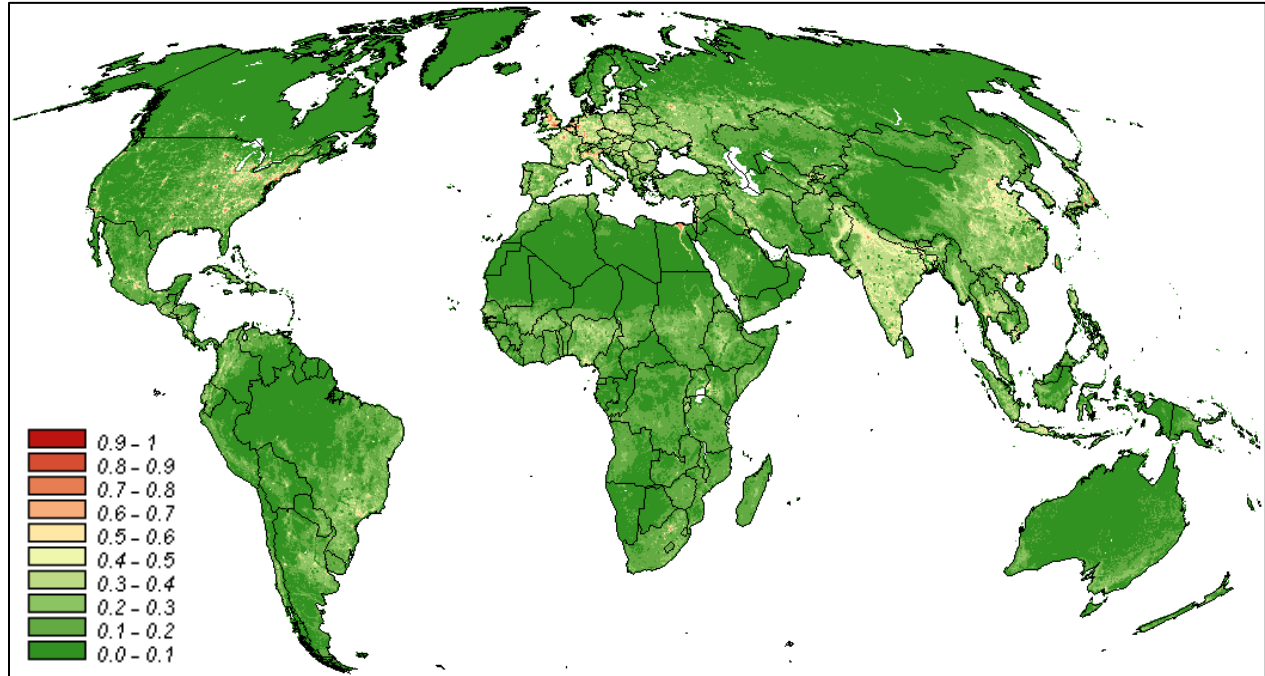
Figure 9. Normalized HF map 2009 displayed in equal interval bins.

Direct map comparison

Based on a cell-by-cell comparison, HM_c values and normalized HF scores were strongly correlated (Pearson's $r = 0.77$). Based on visual assessment, each map has the majority of cells scored ≤ 0.4 (as shown in green hues), but differences occurred at higher values (as shown in red hues). This was further illustrated when examining cell counts in each 0.1 bin (Table 3): in which there were similar cell percentages in the 0.0-0.4 bins across the two maps, but 2x-8x more cells in the HM_c 0.4-1.0 bins relative to HF. Further, at a global scale, absolute HM_c values tended to be higher than HF values (HM_c mean $\pm 1SD = 0.19 \pm 0.22$, HM_c median $= 0.10$; HF mean $= 0.12 \pm 0.14$, HF median $= 0.08$) (Table 4).

Table 3. Cell distributions of HM_c and normalized HF using equal interval bins. (Note that Categories are greater than first number and less than or equal to the last (e.g., > 0.1 - ≤ 0.2), except for the $0.0 – \leq 0.1$ bin, which includes zero values.)

Category Bin	HM_c Cell Count	HM_c Percent Total	HF Cell Count	HF Percent Total
0.9 – 1.0	155,482	0.117%	107,339	0.081%
0.8 – 0.9	703,625	0.528%	271,162	0.204%
0.7 – 0.8	4,595,111	3.45%	570,012	0.428%
0.6 – 0.7	6,595,461	4.952%	985,949	0.740%
0.5 – 0.6	4,750,620	3.567%	1,409,378	1.058%
0.4 – 0.5	5,659,328	4.249%	2,823,900	2.120%
0.3 – 0.4	7,525,638	5.651%	7,258,656	5.450%
0.2 – 0.3	12,847,558	9.647%	15,304,394	11.491%
0.1 – 0.2	24,965,311	18.745%	28,461,076	21.370%
0.0 – 0.1	65,383,849	49.094%	75,990,117	57.057%

Table 4. Global statistics for HM_c and normalized HF. Note that these numbers may differ from published values due to this comparison being restricted to only overlapping cells.

Analysis	Mean	1 STD	Median	1 MAD
HM_c	0.19	0.22	0.10	0.10
HF	0.12	0.14	0.08	0.11

Comparison of score differences

Similar differences can be seen when we examined the differences between the two maps (i.e., HM_c - normalized HF) (Fig. 10). Although ~70% of cells had absolute differences ≤ 0.1, ~25% of comparable cells had higher HM_c values relative to only 5% HF cells (Table 5). The greatest pixel-level differences were in parts of North America, Europe, South and Southeast Asia, central Africa and Australia (Fig. 10).
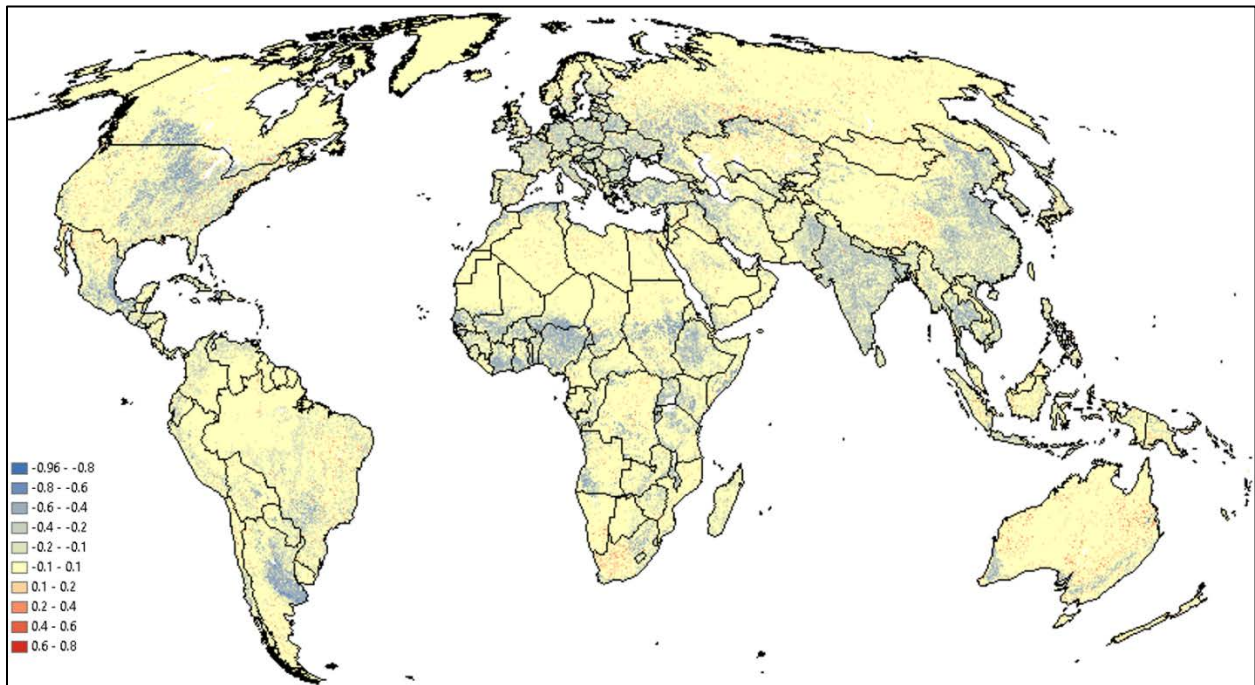

Figure 10. Difference map based on subtracting HM_c from HF. Cooler colors (blue and green) indicate higher HM_c values; warm colors (orange and red) indicate higher HF values; and yellow indicates cells with absolute differences of less than one.

Table 5. Distribution of cells based on subtracting HM_c from HF. Binning and colors match the legend in the Fig. 11 map. Values in parentheses indicate negative values.

Category	Cell Count	Percent Total	
< (0.8)	6,464	0.00%	HM Higher
(0.8) – (0.6)	191,343	0.14%	HM Higher
(0.6) – (0.4)	6,017,071	4.52%	HM Higher
(0.4) – (0.2)	12,574,044	9.44%	HM Higher
(0.2) – (0.1)	14,128,984	10.61%	HM Higher
(0.1) – 0.1	93,809,171	70.44%	
0.1 – 0.2	5,523,682	4.15%	HF Higher
0.2 – 0.4	919,517	0.69%	HF Higher
0.4 – 0.6	11,660	0.01%	HF Higher
>0.6	47	0.00%	HF Higher

Higher HM_c values were due to differences between how the two analyses calculated cumulative scores (i.e., HM_c using a fuzzy sum algorithm and HF using simple addition). For example, a cell that both datasets identified as having 100% cropland as the sole stressor had two very different values (i.e., HM_c ~0.7 and HF 0.14). Similarly, an area fully built-up had HM_c values ~1.0, whereas HF scores would only be close to 1 in cases where human population density, built-up, and night-time lights had maximum scores of 10 each and at least two of three additional features (e.g., roads, railways, and/or navigable waters) also overlapping. Without these pressures in addition to population density, built-up and night-time lights, the maximum value would be 0.6 (i.e., 30/50). Of note, this score would be similar to those designated as cropland within the HM_c. Extreme HM_c values greater than HF (i.e., -0.8) were detected to be mining areas with 2013 night-time lights overlapping within the HM_c that went undetected by the 2009 night-time lights used by the HF.

Higher HF values tended to be cells with major roads or railroads intersecting them, without any other pressures. Differences related to how cells were scored for those stressors. For example, cells where roads intersected within the HF were always scored at 0.16 (i.e., 8/50). In contrast, within the HM_c, the footprint of a major road was estimated and then multiplied by an estimated intensity; e.g., 1 km of road with a width estimate of 30 m produced a footprint of 0.03 km^2 and multiplied by an intensity of 0.83 to derive a final score of 0.0249. Where HF scores were greater than 0.4, they tended to be areas where the 2009 night-time lights intersected roads and these lit areas were not present with the 2013 night-time lights data used in the HM_c.

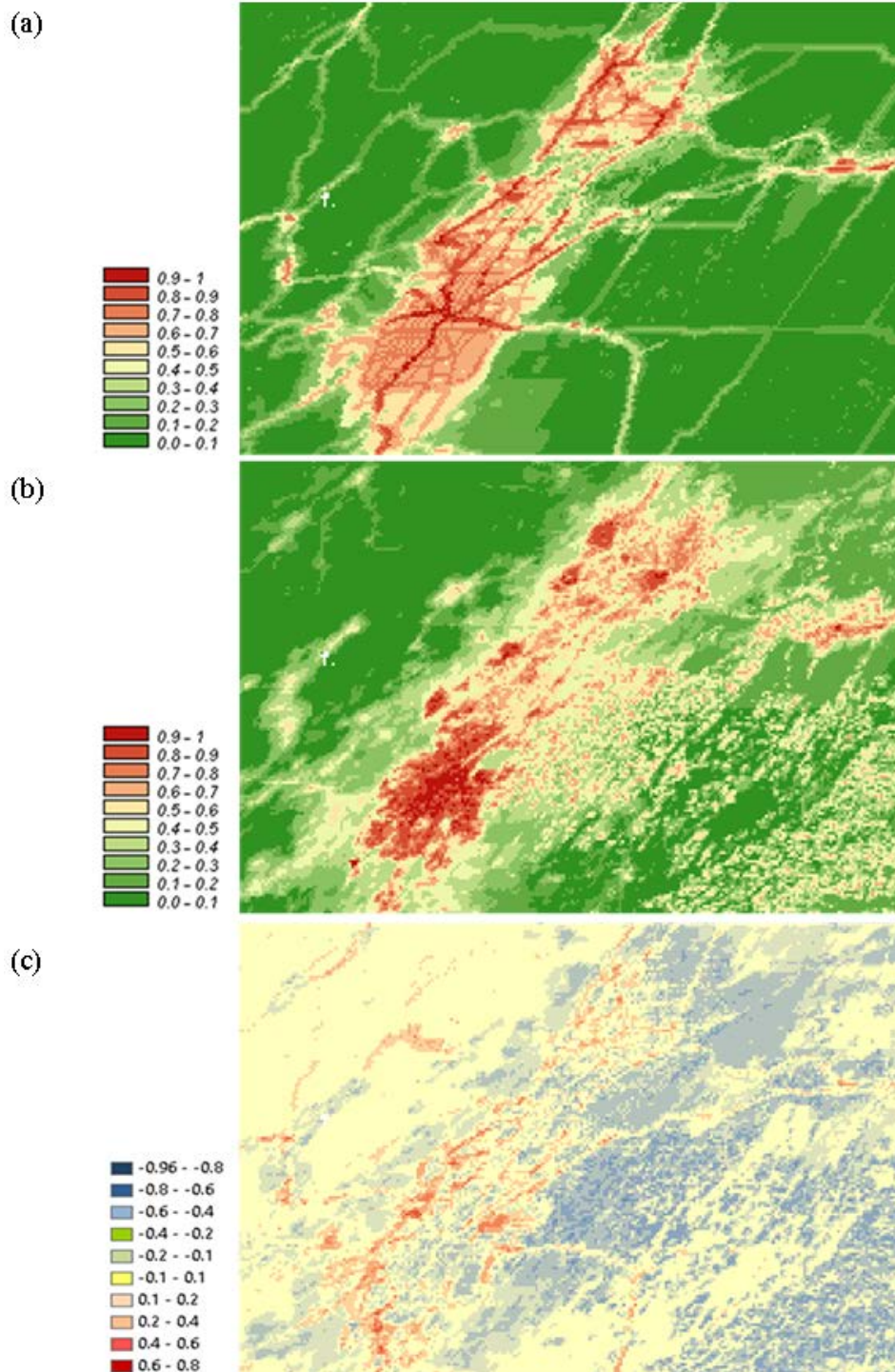*Comparison of regional-level differences*

Figure 11. Comparison of scores for Denver, Colorado, USA for (a) HM_c map, (b) Normalized 2009 HF map, and (c) Differences based on subtracting HM_c from normalized HF. Cool colors (blue and green) indicate higher HM_c values; warm colors (orange and red) indicate higher HF values; and yellow color indicates cells with absolute differences of less than one.

Comparison of areas mapped with no human influence
In previous analyses, HF was used to identify areas devoid of human pressures (termed "wilderness" areas) (i.e., HF = 0) (Watson *et al.*, 2016). Following this categorization, we compared the two maps with reference to their zero values and found that the HF delineated 3.7x more of these areas than the HM. Specifically, HF mapped ~19% of terrestrial lands without human influence (n = 24,744,093) relative to only ~5% by the HM_c map (n = 6,697,770 cells) (Fig. 12).[8] Further, there was only a 21% overlap between the areas mapped as having no influence by these two maps. When examining those cells with no HF stressors mapped but with HM stressors, the key drivers were human population (57% of cells) and livestock (42% of cells) datasets (Table 6). Conversely those cells with no HM stressors but with HF pressures, the main drivers were navigable waters (47% of cells), human population (22%), roads (21%), and pasture (9%) (Table 7).
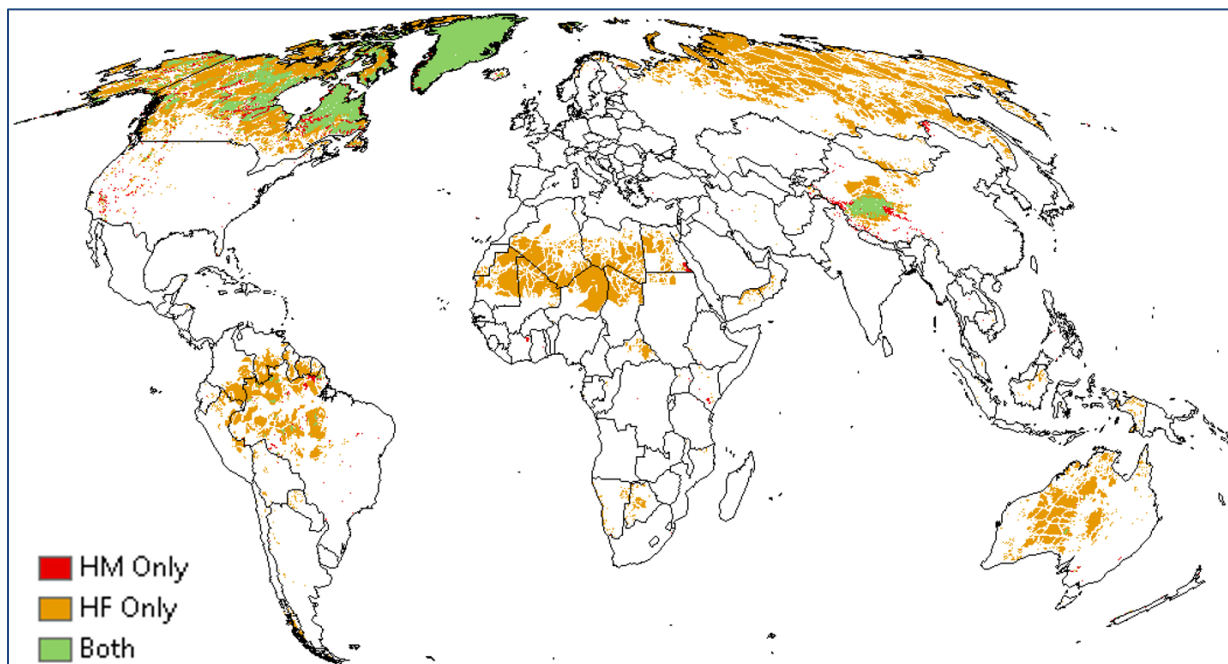

Figure 12. Areas mapped with no human pressures or stressors (i.e., HM_c or HF = 0). Green indicates cells where both maps identified the same cells as zero (n = 5,501,167), red indicates where only HM_c cells had zero values (n = 1,196,603), and orange indicates where only HF cells had zero values (n = 19,242,926).

---

[8] Note that these numbers may differ from published values due to this comparison being restricted to only overlapping cells.

Table 6. Statistics for non-zero HM_c values that overlapped HF zero cells. "Category" identifies those HM_c stressors that contributed the most to the cumulative HM_c score and had the highest percentage of overlap (i.e., %) with HF zero values.

Category	%	# of Cells	Min	Max	Median	95th Percentile	Mean	STD
Population	57	11,006,101	0.000001	0.449686	0.006407	0.061772	0.015404	0.023119
Livestock	42	8,040,912	0.000001	0.370000	0.003620	0.075340	0.015928	0.030723
Other 10 stressors	1	195,913						
HM	100	19,242,926	0.000001	0.946632	0.004562	0.059508	0.014436	0.029105

Table 7. Statistics for non-zero HF scores that overlapped HM_c zero cells. "Category" identifies those HF stressors that contributed the most to the cumulative HF score and had the highest percentage of overlap (i.e., %) with HM_c zero values. All values were rescaled from 0-1.

Category	%	# of Cells	Min	Max	Median	95th PCTL	Mean	STD
Navigable Water	47	555,992	0.000943	0.08	0.04464	0.08	0.042963	0.02345
Population	22	267,019	0.02	0.2	0.02	0.08	0.035138	0.0244
Roads	21	251,989	0.005	0.16	0.0051	0.08	0.013726	0.02307
Pasture	9	112,750	0.02	0.08	0.04	0.06	0.034955	0.01606
Other 4 pressures	1	8,853						
HF	100	1,196,603	0.000943	0.5600	0.03510	0.10197	0.042346	0.03605

Comparison by biome, ecoregion, and country
Comparisons at a biome, ecoregion, and country level showed a similar pattern as the global scale: i.e., highly correlated values but higher overall HM_c values relative to normalized HF scores. At the biome scale, mean and median HM_c and normalized HF values were strongly correlated ($r = 0.98$ for both). At the biome scale, only the desert biome had a slightly higher HF median score than that of HM_c (Fig. 13, Table 8). This was due to mainly to the HF mapping both direct and indirect effects of roads. Both datasets identified the same biomes as being the top five most modified (i.e., Temperate Broadleaf and Mixed Forest; Tropical and Subtropical Dry Broadleaf Forest; Mediterranean Forest, Woodland, and Scrub; Mangroves; Temperate Grasslands, Savannas, and Shrublands) and least modified (i.e., Tundra, Boreal Forest/Taiga, Deserts and Xeric Shrublands, and Temperate Coniferous Forests). Differences in median scores were higher for the highest modified biome: Temperate Broadleaf and Mixed Forests had the largest median score difference of 0.1556. This difference was pronounced because this biome had the highest amount of area identified as cropland (i.e., 3,523,999 km^2 equal to 23% of the global cropland total) and urban (i.e., 335,108 km^2 equal to 44% of the global settlement areas).

Similar to the biome scale, mean and median ecoregion scores were highly correlated ($r = 86$ and 0.85, respectively), but estimated to be higher by the HM_c relative to the HF. Specifically, 622 of 819 ecoregions (or 76%) had higher median HM_c values (Fig. 14). 241 of these 622 ecoregions (or 29%) had median score differences greater than 0.1. The *Veracruz Dry Forests* ecoregion exhibited the highest median difference of 0.57, which was due to intensive cropland conversion undetected by the GlobCov data used in the HF analysis. In contrast, only 7 ecoregions had higher median HF scores greater than 0.1 relative to the HM_c. The *New Caledonia dry forests* ecoregion had a HF median value 0.206 higher than the HM_c median value, which we suspect is because the Unified Cropland Layer used in the HM_c analysis failed to identify cropland that was mapped by GlobCov.

Lastly, mean and median country-level scores were also highly corrected ($r = 86$ and 0.83, respectively), but estimated to be higher by the HM_c dataset (Fig. 15). 183 of 250 countries (or 73%) had higher HM_c median scores relative to the HF. El Salvador exhibited the highest overall median difference of 0.42. This difference was due to a higher spatial distribution of cropland being identified by the Unified Cropland Layer used within the HM_c relative to the GlobCov used within the HF. Only eight countries had higher HF median scores, all which were islands. This difference again likely contributed to differences in the cropland datasets, the inclusion of the navigable waters along coastlines, and the mapping of roads.
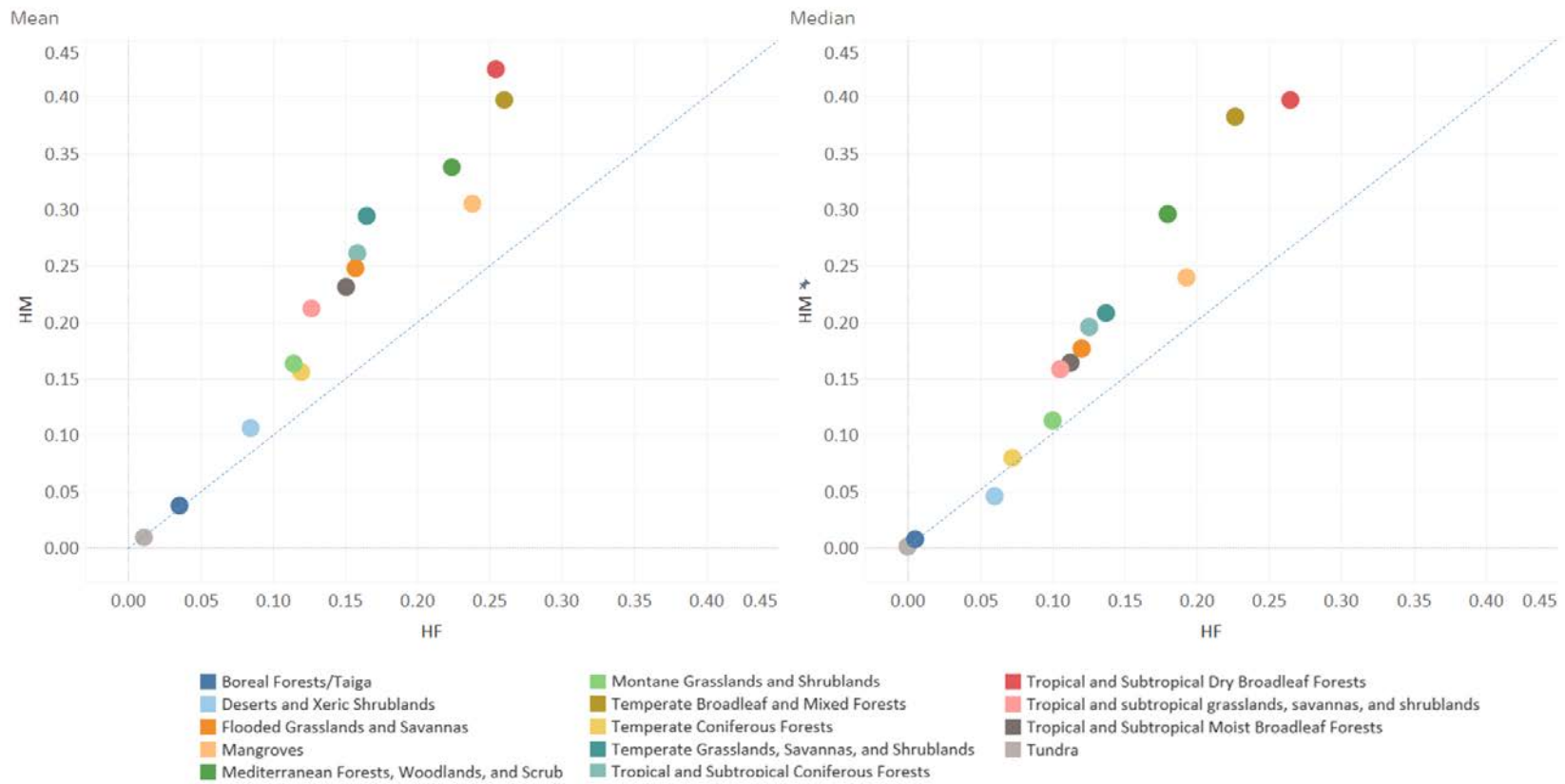
Figure 13. Comparison of HM_c and normalized HF mean and median scores by biome. Dashed blue line indicates the 1:1 line.

Table 8. *HM$_c$* and normalized HF statistics by biome. Modified zScores based on the global median and MAD of each map.

| Biome Name	Mean HM	STD HM	Max HM	Median HM	MAD HM	Modified zScore HM	Mean HF	STD HF	Max HF	Median HF	MAD HF	Modified zScore HF
Boreal Forests/Taiga	0.0374	0.0814	0.9935	0.0073	0.0073	-0.6617	0.0355	0.0736	1.0000	0.0050	0.0074	-0.6745
Deserts and Xeric Shrublands	0.1059	0.1576	0.9950	0.0451	0.0405	-0.4036	0.0848	0.1069	1.0000	0.0600	0.0802	-0.1799
Flooded Grasslands and Savannas	0.2480	0.2066	0.9943	0.1762	0.0725	0.4928	0.1571	0.1479	1.0000	0.1200	0.0885	0.3597
Mangroves	0.3051	0.2237	0.9953	0.2394	0.1309	0.9244	0.2383	0.1574	1.0000	0.1927	0.1151	1.0131
Mediterranean Forests, Woodlands, and Scrub	0.3373	0.2413	0.9964	0.2957	0.1914	1.3088	0.2241	0.1730	1.0000	0.1800	0.1388	0.8993
Montane Grasslands and Shrublands	0.1634	0.1771	0.9936	0.1125	0.0834	0.0570	0.1147	0.1037	1.0000	0.1000	0.1098	0.1799
Temperate Broadleaf and Mixed Forests	0.3968	0.2426	0.9975	0.3820	0.2078	1.8987	0.2600	0.1898	1.0000	0.2264	0.1685	1.3163
Temperate Coniferous Forests	0.1561	0.1797	0.9937	0.0795	0.0674	-0.1686	0.1199	0.1453	1.0000	0.0726	0.0890	-0.0666
Temperate Grasslands, Savannas, and Shrublands	0.2943	0.2299	0.9977	0.2080	0.1405	0.7097	0.1652	0.1315	1.0000	0.1371	0.1068	0.5131
Tropical and Subtropical Coniferous Forests	0.2606	0.1875	0.9895	0.1952	0.0954	0.6222	0.1588	0.1183	0.9200	0.1256	0.0885	0.4101
Tropical and Subtropical Dry Broadleaf Forests	0.4242	0.2360	0.9962	0.3968	0.2202	2.0002	0.2541	0.1475	1.0000	0.2650	0.1557	1.6637
Tropical and subtropical grasslands, savannas, and shrublands	0.2120	0.1925	0.9961	0.1583	0.0840	0.3703	0.1265	0.0950	1.0000	0.1055	0.0808	0.2294
Tropical and Subtropical Moist Broadleaf Forests	0.2310	0.2155	0.9965	0.1638	0.1134	0.4076	0.1509	0.1424	1.0000	0.1126	0.1297	0.2931
Tundra	0.0093	0.0372	0.9596	0.0006	0.0006	-0.7073	0.0111	0.0359	0.9888	0.0000	0.0000	-0.7195
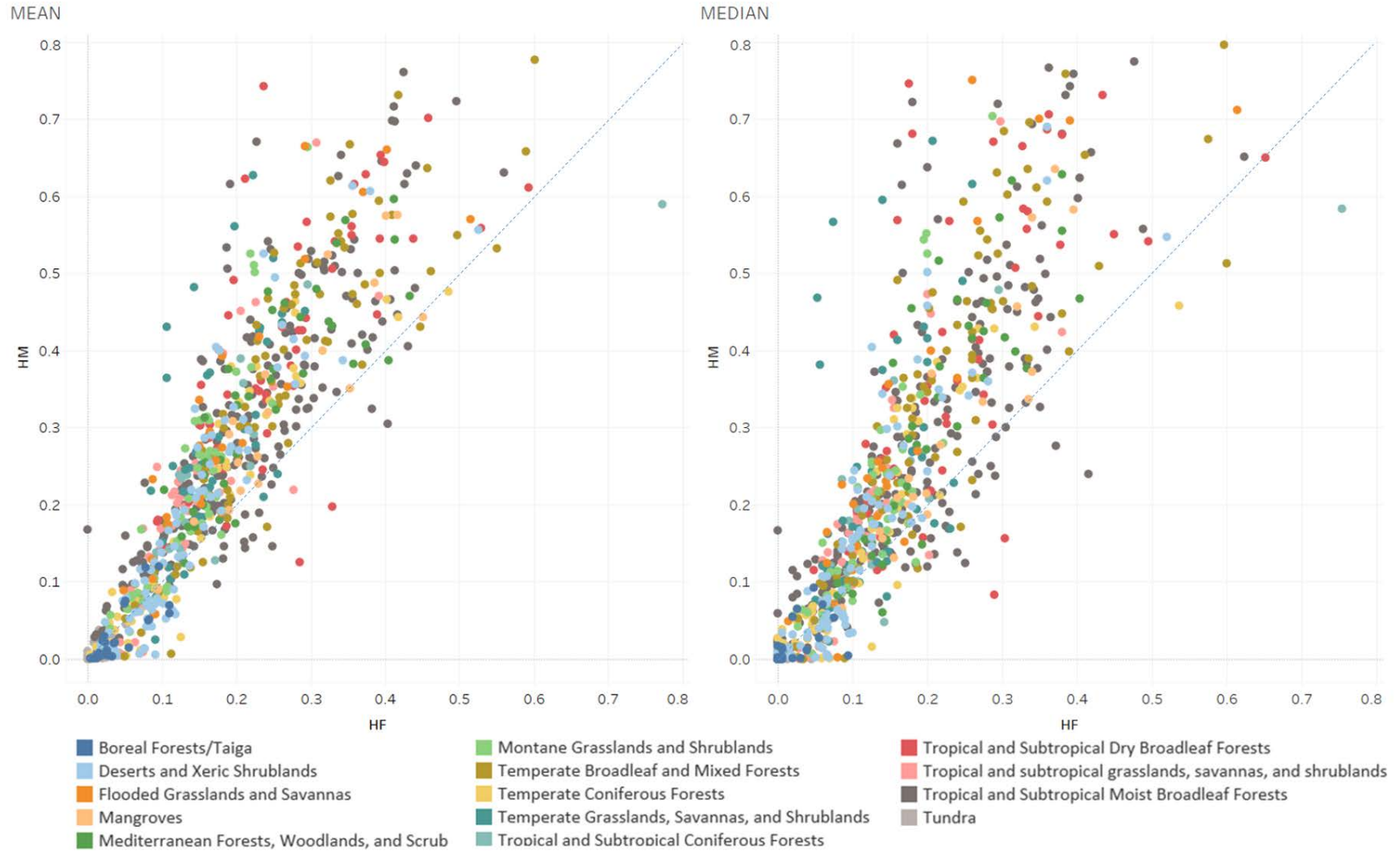
Figure 14. Comparison of HM_c and normalized HF mean and median scores by ecoregion. Dashed blue line indicates the 1:1 line.
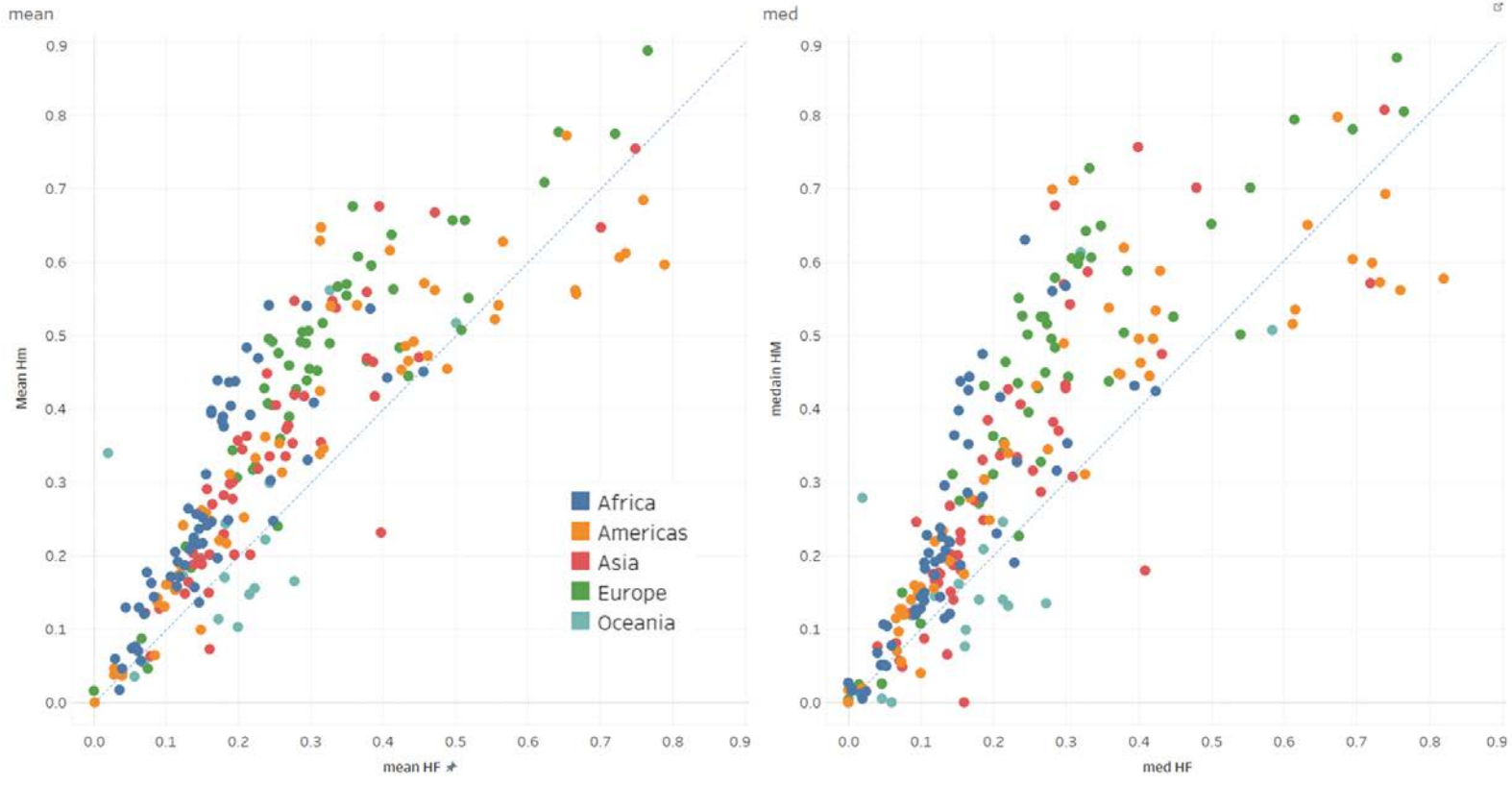
Figure 15. Comparison of HM_c and normalized HF mean and median scores by country. color-coded by geographical regions. Dashed blue line indicates the 1:1 line.

Comparison of *HM_c* values and original HF scores

We also compared these two maps based on their original values and binned by none (no presence of stressor), low, moderate, high, and very high. For the HM_c, these classes were defined as 0.00, $0.00 < HM_c \leq 0.10$, $0.10 < HM_c \leq 0.40$, $0.40 < HM_c \leq 0.70$, and $0.70 < HM_c \leq 1.00$. Low modification was ascribed to areas with median HM_c values on the lower half of the distribution globally (≤ 0.1). Moderate modification ascribed those areas with median HM_c values on the higher half of the distribution globally but not greater than 0.4. We used $HM_c = 0.4$ to demarcate a transition from a moderate to a highly-modified state, because it matches the critical habitat threshold of ~0.60 based on percolation theory (Gustafson & Parker, 1992) and corresponds to low intensity agriculture in our assessment. High to very high breakpoint (0.7) was based on equal binning of the interval values in a manner consistent with empirical syntheses (Alkemade *et al.*, 2009, Brown & Vivas, 2005). For the HF, we used the classes that were defined as 0, $0 < HF \leq 2$, $2 < HF \leq 6$, $6 < HF \leq 12$, and $12 < HF \leq 50$ based on each bin covering 20% of the land surface following Venter *et al.* (2016a).

We calculated the distribution of the terrestrial land surface that fell within these 5 classes at a global scale, and found that a higher percentage of land was classified as highly or very highly modified by HF (37%) relative to the HM_c (17%) (Figure 16). In contrast, the HM_c map had a greater percentage of land classified as low modification (44%) relative to the HF map (16%), while at the same time, had a lower percentage of land without any mapped human stressor (HM_c = 5% vs. HF = 19%).

(a)

Very High (4%)
High (13%)
Moderate (34%)
Low (44%)
None (5%)

(b)

Very High (16%)
High (21%)
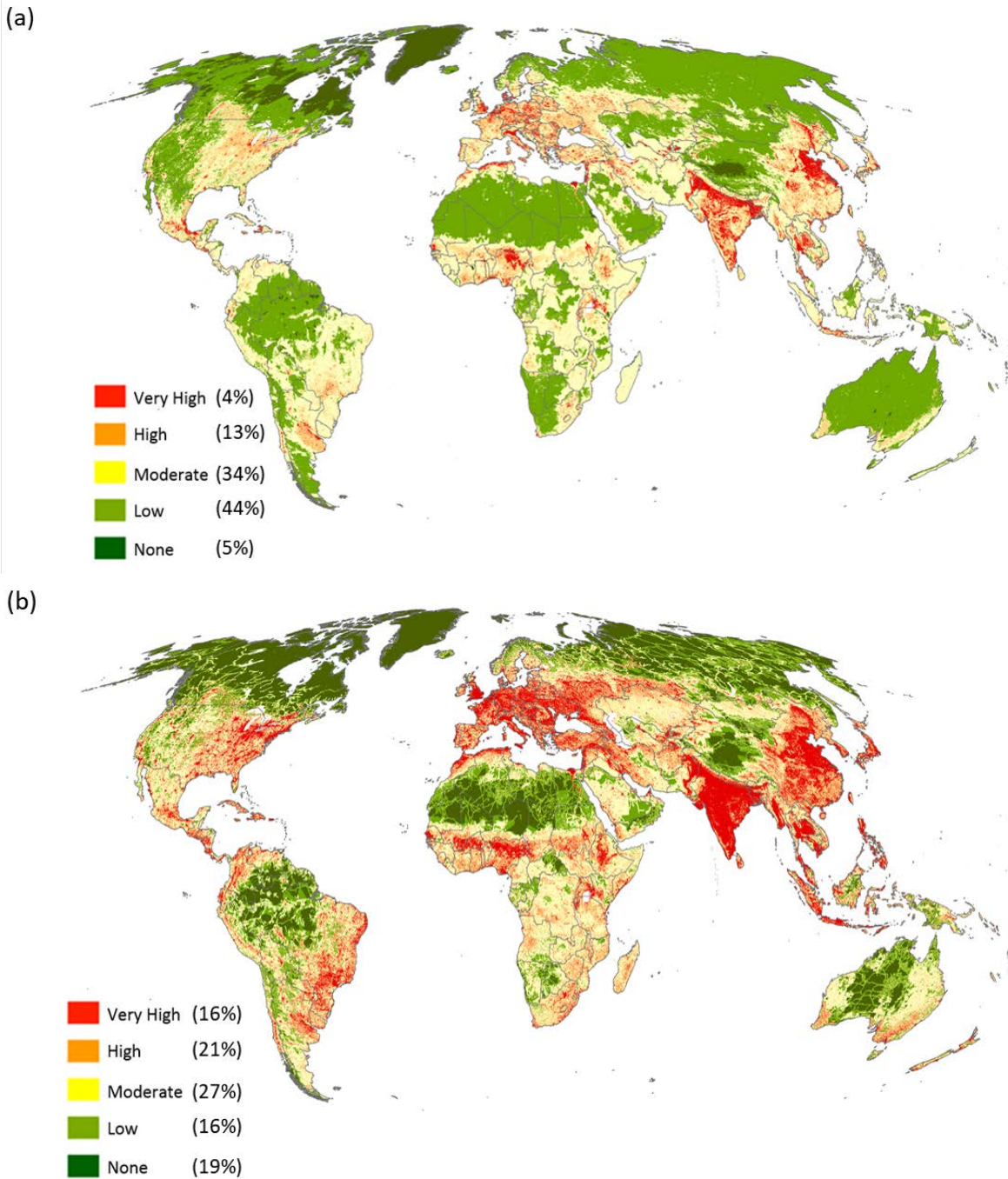Moderate (27%)
Low (16%)
None (19%)

Figure 16. Percentage of land in none, low, moderate, high, and very high classes for (a) the HM_c map based on none = 0.00, low = $0.00 < HM_c \leq 0.10$, moderate = $0.10 < HM_c \leq 0.40$, high $0.40 < HM_c \leq 0.70$, and very high = $0.70 < HM_c \leq 1.0$; and (b) the 2009 HF map based on none = 0, low = $0 < HF \leq 2$, moderate = $2 < HF \leq 6$, high = $6 < HF \leq 12$, and very high = $12 < HF \leq 50$.

We also determined an ecoregional classification into these same 5 bins based on median HM_c and mean HF scores (following each study's protocol). The HF map classified 72% of ecoregions as either highly modified (41%) or very highly modified (31%) relative to only 18% by the HM_c map (Figure 17). In contrast, the HM_c map classified most ecoregions as moderately modified (52%), and secondarily as low or no modification (30%). Thus, the range of map values and how they were binned had substantial effects on the classification of terrestrial lands and ecoregions as human modified by the HM_c and the HF.
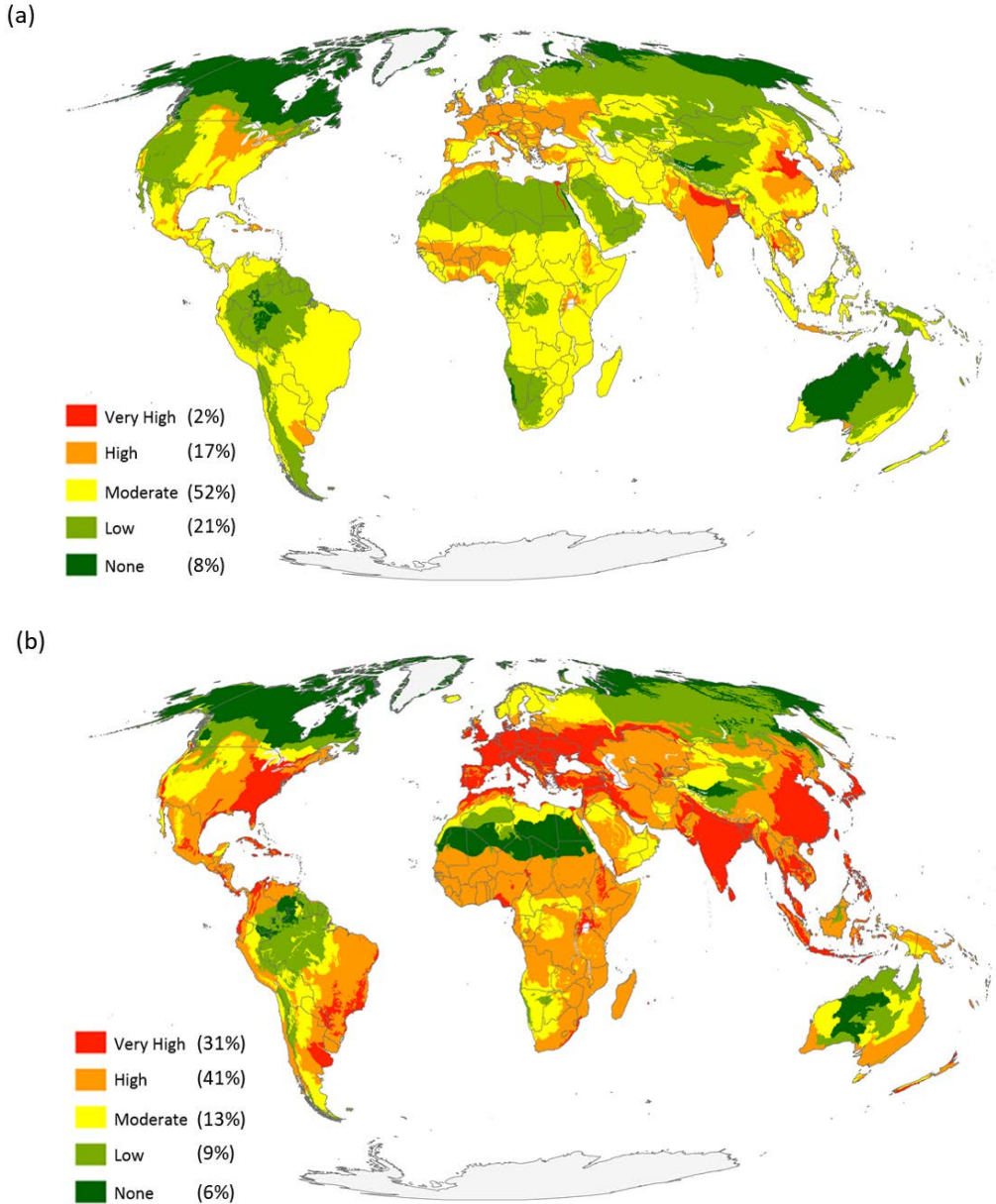
(a)

	Very High	(2%)
	High	(17%)
	Moderate	(52%)
	Low	(21%)
	None	(8%)

(b)

	Very High	(31%)
	High	(41%)
	Moderate	(13%)
	Low	(9%)
	None	(6%)

Figure 17. Percentage of ecoregions in low, moderate, high, and very high classes for (a) the HM_c map based on none = 0.00, low = 0.00 < median $HM_c \leq 0.10$, moderate = 0.10 < median $HM_c \leq 0.40$, high 0.40 < median $HM_c \leq 0.70$, and very high = 0.70 < median $HM_c \leq 1.0$; and (b) the 2009 HF map based on none = 0, low = 0 < mean HF $\leq$ 2, moderate = 2 < mean HF $\leq$ 6, high = 6 < mean HF $\leq$ 12, and very high = 12 < mean HF $\leq$ 50.

To evaluate differences at a sub-ecoregional level, we compared the HM_c and HF score distributions, calculated on Pearson's correlation on the values, and quantified the percentage overlap for cells that were identified as having either none (value = 0 for both maps) or low stress ($HM_c > 0.00\text{-}0.10$ or HF = $> 0\text{-}2$). This ecoregional comparison was done for the 10 target ecoregions classified as moderately modified by the HM_c map.

Despite high correlations between the HM_c values and the normalized HF scores aggregated at broad scales (i.e., global, biome, ecoregion, and country) (as described in sections above), the spatial distributions at smaller, ecoregional scales varied more substantially (Figures 18-19). The correlation between the map scores were lower than found at the global scale ($r = 0.77$), ranging from $r = 0.22 - 0.67$, with exception of one ecoregion (*Everglades flooded grasslands*). The overlap between low modified lands also varied widely, ranging from 0.04% to 64% overlap. These findings are consistent with the low overlap (21%) found between areas mapped to have no human stressor at a global scale by the two maps (as described above).

When comparing ecoregions with a similar percentage of low modified lands but a different degree of fragmentation, ecoregions with a higher degree of fragmentation consistently exhibited a greater difference between the two maps (Figure 19). The *Sierra Madre Occidental pine-oak forests* and *Cardamon Mountain rainforests* ecoregions had a similar amount of low modified lands based on the HM_c map (27% and 21%, respectively), but the former was more fragmented than the latter (1.5km and 4.1 km edge distance, respectively). Consequently, the spatial association between the HM_c map and the HF map was 2 times lower for the *Sierra Madre Occidental pine-oak forests* ($r = 0.40$, 15% overlap) than for the *Cardamon Mountain rainforests* ($r = 0.67$, 30% overlap). Similarly, the *Zambezian Baikiaea woodlands* and the *Sahelian Acacia savanna* ecoregions had the same amount of low modified lands (41%), but the former was more fragmented than the latter (1.1 km and 23.0 km edge distance, respectively). Consequently, the spatial association between the HM_c map and the HF map was 3 times lower for the *Zambezian Baikiaea woodlands* ($r = 0.22$, 36.33% overlap) relative to the *Sahelian Acacia savanna* ($r = 0.64$, 64.21% overlap). Further, the ecoregion with the highest amount of fragmentation, *Maranhão Babaçu forests* (0.4 km edge distance) had the lowest percentage overlap in low modified lands (0.34%).

Finally, we compared the delineation of low modified fragments by each map ($0.00 < HM_c \leq 0.10$ or $0 < HF \leq 2$). To do so, we created a binary raster of low modified lands (coded as value of 1) vs. matrix areas (coded as null values) and then calculated the area of patches (in km^2) using RegionGroup based on an eight-neighbor rule in ArcGIS v10.4 Spatial Analyst extension. Alongside low ecoregional overlap of low modified lands, we found differences in the number and the patch size distributions. Specifically, the HM_c map delineated 2.3x more low modified fragments than the HF map (104,410 vs. 45,905, respectively) (Figure 20). Of the fragments delineated, the HM_c map had a greater percentage of small fragments (≤ 5 km^2) (77%) relative to the HF map (43%); whereas the HF map had a greater percentage of larger fragments (>100 km^2) (25%) relative to the HM_c map (~3%). The reduced delineation of fragments and the bias toward larger patches by the HF is likely due to the buffering of roads and waterways. Collectively, these findings indicate that the degree of human modification and their spatial configurations differ between these two maps at regional scales.
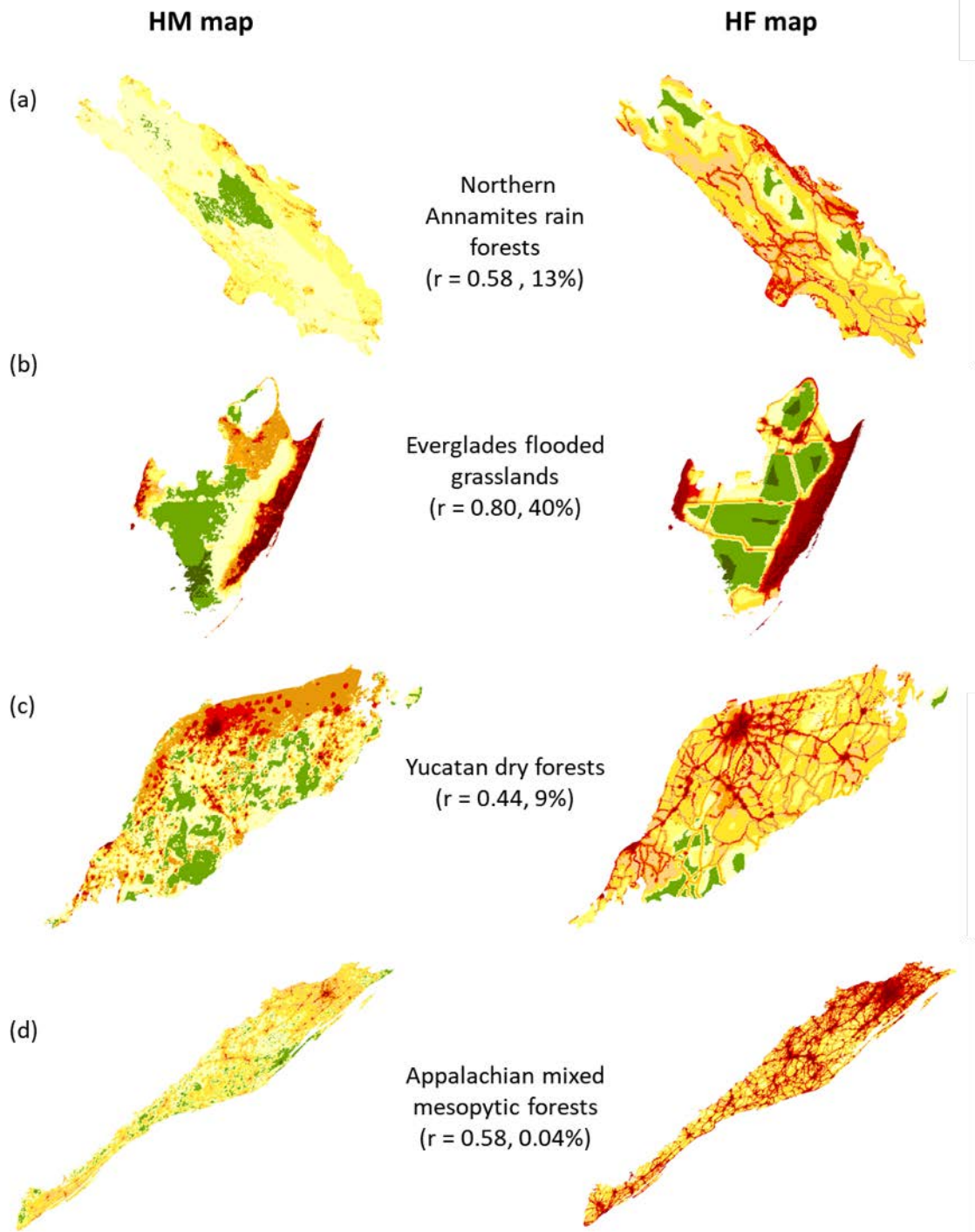
Figure 18. Comparison of the spatial patterns produced by the HM_c map (left) relative to the HF map (right) for representative ecoregions classified as moderately modified by the HM_c map. Pearson's correlations and the percentage of overlap of low modified lands are shown in parentheses.
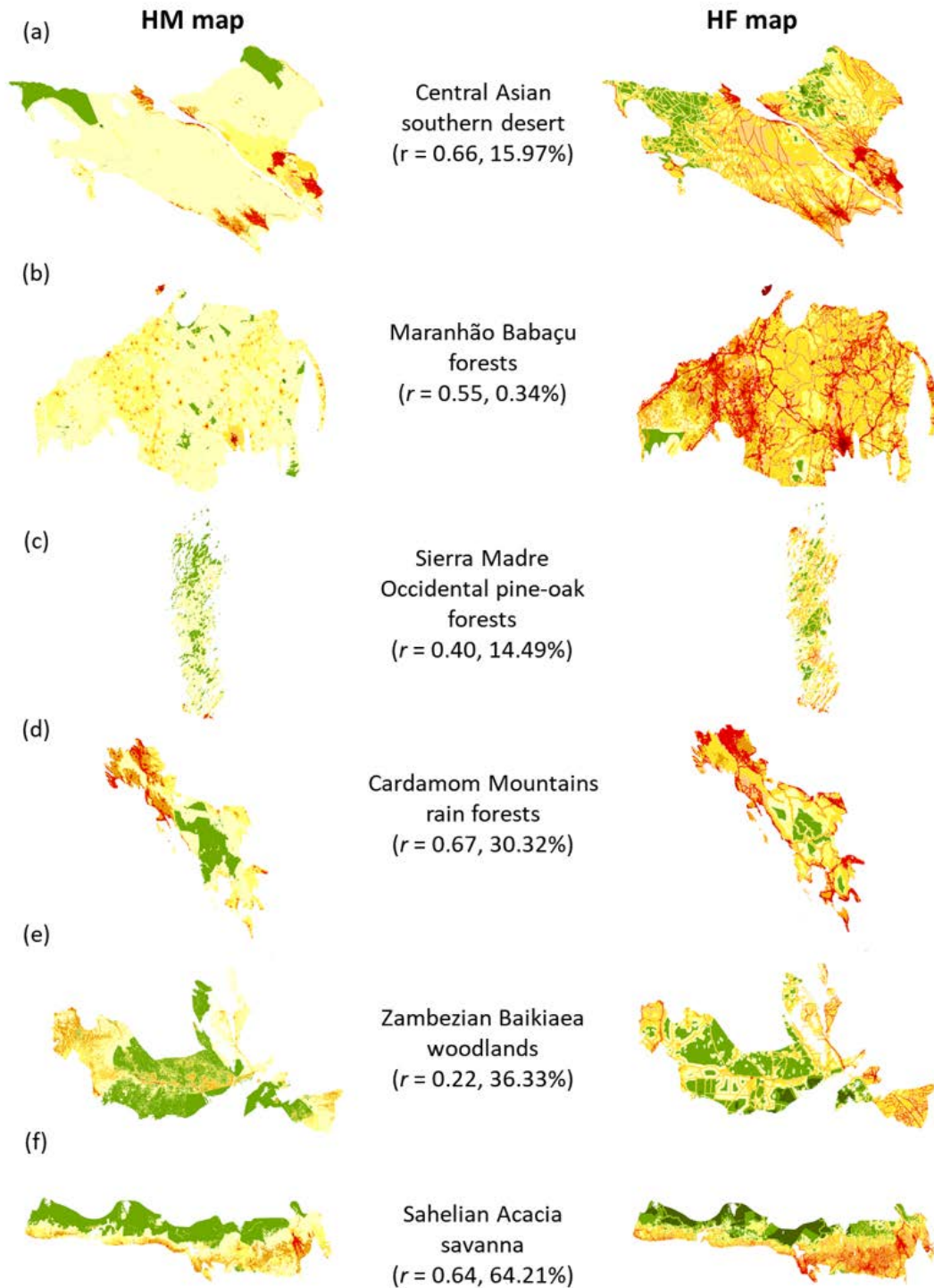
Figure 19. Comparison of the spatial patterns produced by the HM_c map (left) relative to the HF map (right) for representative ecoregions classified as moderately modified by the HM_c map. Pearson's correlations and the percentage of overlap of low modified lands are shown in parentheses.
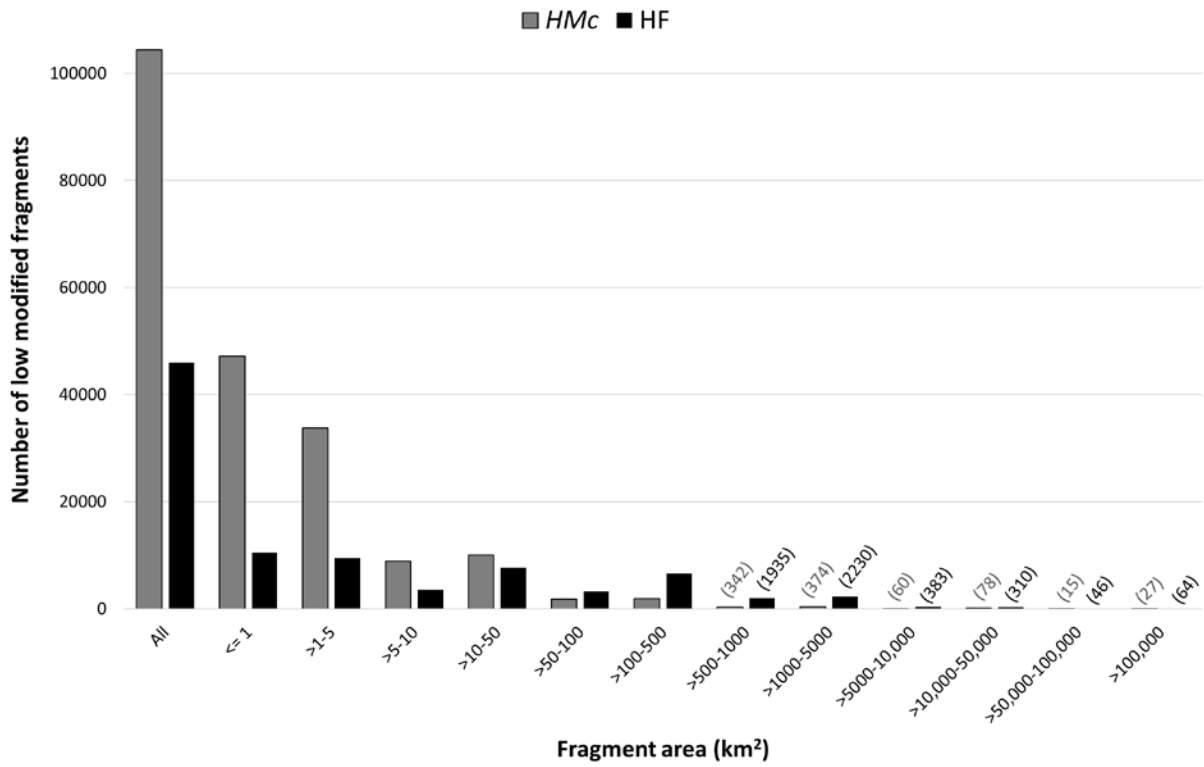
Figure 20. The number of low modified fragments ($0.00 < HM_c \leq 0.10$ or $0 < HF \leq 2$) and their patch size distributions delineated by the HM_c map (grey) relative to the HF map (black).

References

Alkemade R, Van Oorschot M, Miles L, Nellemann C, Bakkenes M, Ten Brink B (2009) GLOBIO3: a framework to investigate options for reducing global terrestrial biodiversity loss. Ecosystems, **12**, 374-390.

Bonham-Carter GF (1994) *Geographic Information Systems for geoscientists: Modeling with GIS,* Pergamon, Oxford, Elsevier.

Brown MT, Ulgiati S (2002) Emergy evaluations and environmental loading of electricity production systems. Journal of Cleaner Production, **10**, 321-334.

Brown MT, Vivas MB (2005) Landscape development intensity index. Environmental Monitoring and Assessment, **101**, 289-309.

Center for International Earth Science Information Network - Ciesin - Columbia University and Information Technology Outreach Services - Itos - University of Georgia (2013) Global Roads Open Access Data Set, version 1 (gROADSv1). Palisades, NY, NASA Socioeconomic Data and Applications Center (SEDAC).

Crain CM, Kroeker K, Halpern BS (2008) Interactive and cumulative effects of multiple human stressors in marine systems. Ecology Letters, **11**, 1304-1315.

Darling ES, Côté IM (2008) Quantifying the evidence for ecological synergies. Ecology Letters, **11**, 1278-1286.

Doxsey-Whitfield E, Macmanus K, Adamo SB, Pistolesi L, Squires J, Borkovska O, Baptista SR (2015) Taking advantage of the improved availability of census data: A first look at the Gridded Population of the World, version 4. Papers in Applied Geography, **1**, 226-234.

Elvidge CD, Imhoff ML, Baugh KE *et al.* (2001) Night-time lights of the world: 1994–1995. ISPRS Journal of Photogrammetry and Remote Sensing, **56**, 81-99.

European Space Agency (2011) GlobCover Land Cover V2.3 ESA, led by MEDIAS.

Gustafson EJ, Parker GR (1992) Relationships between landcover proportion and indices of landscape spatial pattern. Landscape Ecology, **7**, 101-110.

Halpern BS, Fujita R (2013) Assumptions, challenges, and future directions in cumulative impact analysis. Ecosphere, **4**, 1-11.

Kennedy CM, Oakleaf JR, Theobald DM, Baruch-Mordo S, Kiesecker J (2018) Global Human Modification. https://doi.org/10.6084/m9.figshare.7283087, figshare.

Kennedy CM, Oakleaf JR, Theobald DM, Baruch-Mordo S, Kiesecker J (2019) Managing the middle: A shift in conservation priorities based on the global human modification gradient. Global Change Biology, **12**, 811-826. https://doi.org/810.1111/gcb.14549.

Mcbride MF, Garnett ST, Szabo JK *et al.* (2012) Structured elicitation of expert judgments for threatened species assessment: a case study on a continental scale using email. Methods in Ecology and Evolution, **3**, 906-920.

National Imagery and Mapping Agency (1992) VMAP_1V10 - Vector Map Level 0 (Digital Chart of the World).

Openstreetmap Contributors (2016) OpenStreetMap, the Free WikiWorld Map. Retrieved from www.openstreetmap.org.

Perkl RM (2017) Measuring landscape integrity (LI): development of a hybrid methodology for planning applications. Journal of Environmental Planning and Management, **60**, 92-114.

Pesaresi M, Huadong G, Blaes X *et al.* (2013) A global human settlement layer from optical HR/VHR RS data: Concept and first results. IEEE Journal of Selected Topics in Applied Earth Observations and Remote Sensing, **6**, 2102-2131.

Ramankutty N, Evan AT, Monfreda C, Foley JA (2008) Farming the planet: 1. Geographic distribution of global agricultural lands in the year 2000. Global Biogeochemical Cycles, **22**, GB1003-GB1003.

Robinson TP, William Wint GR, Conchedda G *et al.* (2014) Mapping the global distribution of livestock. PLoS ONE, **9**, e96084.

Salafsky N, Salzer D, Stattersfield AJ *et al.* (2008) A standard lexicon for biodiversity conservation: unified classifications of threats and actions. Conservation Biology, **22**, 897-911.

Sanderson EW, Jaiteh M, Levy MA, Redford KH, Wannebo AV, Woolmer G (2002) The Human Footprint and the Last of the Wild. Bioscience, **52**, 891-891.

Speirs-Bridge A, Fidler F, Mcbride M, Flander L, Cumming G, Burgman M (2010) Reducing overconfidence in the interval judgments of experts. Risk Analysis, **30**, 512-523.

Theobald D (2016) A General-Purpose Spatial Survey Design for Collaborative Science and Monitoring of Global Environmental Change: The Global Grid. Remote Sensing, **8**, 813.

Theobald DM (2010) Estimating natural landscape changes from 1992 to 2030 in the conterminous US. Landscape Ecology, **25**, 999-1011.

Theobald DM (2013) A general model to quantify ecological integrity for landscape assessments and US application. Landscape Ecology, **28**, 1859-1874.

Theobald DM, Zachmann LJ, Dickson BG, Gray ME, Albano CM, Landau V, Harrison-Atlas D (2016) Description of the approach, data, and analytic methods used to estimate natural land loss in the western U.S. pp 23, https://www.disappearingwest.org/, Conservation Science Partners.

Venter O, Sanderson EW, Magrach A *et al.* (2016a) Sixteen years of change in the global terrestrial human footprint and implications for biodiversity conservation. Nature Communications, **7**, 12558.

Venter O, Sanderson EW, Magrach A *et al.* (2016b) Global terrestrial Human Footprint maps for 1993 and 2009. Scientific Data, **3**, 160067.

Waldner F, Fritz S, Di Gregorio A *et al.* (2016) A unified cropland layer at 250 m for global agriculture monitoring. Data, **1**, 3.

Watson JE, Shanahan DF, Di Marco M *et al.* (2016) Catastrophic declines in wilderness areas undermine global environment targets. Current Biology, **26**, 1-6.